



VAASAN AMMATTIKORKEAKOULU
UNIVERSITY OF APPLIED SCIENCES

Mikko Niemelä

EXPERIMENTAL STRENGTH TESTS WITH METAL X

School of Technology
2020

ABSTRACT

Author	Mikko Niemelä
Title	Experimental Strength Test with Metal X
Year	2020
Language	English
Pages	86
Name of Supervisor	Juha Hantula, Markus Välimäki

This thesis was done for Wärtsilä's New Product Introduction & Smart Manufacturing department. The purpose of this thesis was to find out the impact of basic geometries and plausible influences and restrictions for the strength of the metal samples manufactured with Metal X. Wärtilä's first metal printer MarkForged Metal X was ordered at the end of 2018, and the need for this thesis was because it was a printer with a new printing concept and there was no reference base yet.

In this thesis, the strengths of samples printed with Metal X, and the effects of the infill on the strengths of the samples were studied in three different ways. The parts were designed with NX 3D modelling software, Markforged Eiger software for printers was used to prepare the print, and the pieces were printed with Metal X. Strength tests were performed at Dekra's site and material tests at Wärtsilä Vaasa factories materials research department.

Some of the test results were as expected. For example, the effect of the printing direction to the strength, but the surprise was that the difference was as big as it was. In some cases, the tests failed, and some of the tensile test bars did not break as planned. Overall, however, the results provided an insight into what can be done with pieces printed with Metal X and what tests need to be done in the future if parts are to be used in strength-intensive applications.

Keywords Metal X, additive manufacturing and 3D printing

CONTENTS

TIIVISTELMÄ

ABSTRACT

GLOSSARY

1	INTRODUCTION.....	13
2	WÄRTSILÄ OYJ.....	14
	2.1 From History to Today.....	14
	2.2 Organization and Strategy.....	15
	2.2.1 Wärtsilä Marine Business.....	16
	2.2.2 Wärtsilä Energy Business.....	17
3	METAL ADDITIVE MANUFACTURING.....	18
	3.1 Characteristics of Metal Additive Manufacturing.....	19
	3.1.1 Powder Bed Fusion.....	19
	3.1.2 Binder Jetting.....	22
	3.1.3 Direct Energy Deposition.....	23
	3.1.4 Metal Extrusion.....	24
	3.2 Value of Metal Additive Manufacturing in industry.....	26
	3.2.1 Improved Performance through Design.....	26
	3.2.2 Possibilities of AM.....	28
	3.3 The Future of Additive Manufacturing.....	30
	3.4 Additive Manufacturing in Wärtsilä.....	31
4	METAL FUSED DEPOSITION MODELING.....	33
	4.1 Metal X.....	33
	4.1.1 Materials.....	34
	4.1.2 Print Preparation.....	35
	4.1.3 Print Process.....	37
	4.2 Pros & Cons.....	39
	4.3 Metal X, Commissioning and Factory Assembly.....	42
5	MATERIAL TEST EXPERIMENTS.....	44
	5.1 Strength of the Printed Material.....	48
	5.2 Strength of the Printed Basic Geometry.....	51

5.2.1	Tensile Strength.....	52
5.2.2	3-Point Bending Strength.....	58
5.2.3	Compression Strength.....	63
6	DESIGN FOR ADDITIVE MANUFACTURING FOR ADAM IN STRENGTH PERSPECTIVE	66
6.1.1	Part Dimensions.....	66
6.1.2	Surface Quality.....	67
7	SUMMARY.....	69
8	CONCLUSIONS.....	73
	REFERENCES.....	78

LIST OF FIGURES AND TABLES

Figure 1. Smart Technology Hub. /3/.	14
Figure 2. Wärtsilä's net sales by business in 2018. /4/.	15
Figure 3. Wärtsilä's strategy. /4/.	16
Figure 4. The increase of AM machine manufacturers from 2012 to 2018. /7/.	18
Figure 5. A picture showing Renishaw's PBF print process in action. /9/.	19
Figure 6. The principle of Powder Bed Fusion. /9/.	20
Figure 7. A metal bracket before supports are removed. /11/.	21
Figure 8. Support free bottle opener manufactured with Velo3D. /12/.	22
Figure 9. Binder Jetting printing process. /13/.	23
Figure 10. The principle of Direct Energy Deposition. /14/.	24
Figure 11. The principle of Metal extrusion. /13/.	25
Figure 12. Comparison between metal manufacturing techniques. As it can be seen, every AM method is located where the batch size is smaller, but the complexity of the part is higher /20/.	26
Figure 13. Lattice structure manufactured with PBF. Creating the lattice structure inside the part could help to minimize the weight while retaining the strength. /24/.	27
Figure 14. Lattice structure manufactured inside the chamber by PBF. For example, heat exchangers with optimized geometry for flow rate could gain benefit from this. /24/.	27
Figure 15. General Electric's fuel nozzle, where 20 different part has been consolidated into one with AM. /26/.	28
Figure 16. Different applications and their value drivers. /23/.	29
Figure 17. Solukon powder removal machine. /55/.	31
Figure 18. Fortus 400mc. (Feasibility study for Wärtsilä.)	32
Figure 19. Metal X entity. /30/.	34
Figure 20. Part view page from Eiger, part detail information is on the left, and part settings information is on the right.	35
Figure 21. Part detail window in Eiger.	36

Figure 22. Internal View page, where it can be seen layer by layer how the part will be printed, where support materials, ceramics and materials are printed.	36
Figure 23. The white ceramic release layer, which makes the part release from the raft easier.	37
Figure 24. Schematic representation of the shaping, debinding, and sintering process. /42/.....	39
Figure 25. Same part compared with PBF and Metal X, if printed multiple parts the PBF process is clearly much faster.	40
Figure 26. CT analysis of the same part printed with LB-PBF and Metal FDM. The porosity inside the Metal FDM produced part is significant compared to LB-PBF produced part. /20/.....	41
Figure 27. The infill structure in printing phase is well seen.	41
Figure 28. Pre-combustion run of the sinter before use.	43
Figure 29. The principle of tensile test machine. /52/.....	44
Figure 30. The principle of 3-point bending test. /54/.....	46
Figure 31. The principle of compression test. /55/.....	47
Figure 32. Maximum stress from solid test samples material strength tests.....	49
Figure 33. 1000 μm overview from the cross sections. Sample number one on the left printed August 2018, sample number three on the middle, printed October 2018 and number six on the right, printed September 2019.	50
Figure 34. 100 μm close-up from the cross section. Sample number one on the left, sample number three on the middle and sample number six on the right.....	50
Figure 35. Printed & machined sample to demonstrate the sintered infill.....	51
Figure 36. Weight reduction compared to solid part, which is a result of the infill structure inside the part.	51
Figure 37. Internal view from Eiger, same part as in Figure 20 and in Figure 22 but from the layer 29. The white is the actual part material, the orange is a release material and the grey is a support material.	52
Figure 38. Calculated values based on the Eiger internal view. Two different calculations were made, infill included and not included in calculations.....	53
Figure 39. 20mm x 20mm test sample locations in print bed.	54

Figure 40. Comparison between calculation model and strength test values with samples TS1.....	55
Figure 41. Test sample series TS11, where can be seen that one sample is broken outside the measurement zone, although the strength to break the sample did not deviate from others.	56
Figure 42. Elongation data from TS1-1, -2, and -3 test samples.....	56
Figure 43. The actual and calculated break force for the tensile test samples.	57
Figure 44. Relationship of maximum force and stress with 3-point bending samples.....	57
Figure 45. Printing directions for size 15 mm x 15 mm.	59
Figure 46. Bending direction Z for sample series 3BS1, 3BS3 and 3BS7.....	59
Figure 47. Bending direction Y for sample series 3BS2, 3BS4 and 3BS8.	59
Figure 48. Test sample 3BS8-3 before loading.	60
Figure 49. Test sample 3BS8-3 after loading.....	60
Figure 50. Three-point bending test results.....	61
Figure 51. The breaking load in the 3-point bending test, with 15 mm x 15 mm samples.....	62
Figure 52. Flexural stress compared to cross-section of 3-point bend samples. ..	62
Figure 53. The Young's modulus compared to cross-section of 3-point bend samples.....	63
Figure 54. Compression test samples after the test, CS1 on the left and CS2 on the right.	64
Figure 55. Maximum loads of compression test samples.	64
Figure 56. Compression stress chart for compression test samples in series CS1 and CS2.....	65
Figure 57. The maximum dimensions with Sinter 2 /57/.....	66
Figure 58. Surface roughness test pieces. 0 degree on the left, 45 degree on the middle and 90 degree on right.....	67
Figure 59. Measured Ra and Rz values. On the left Ra values and on the right Rz values.	68

Figure 60. Cross-section views from Eiger, TS1-X on the top and TS1-1 on the bottom. This demonstrates that the infill structure has a huge impact to the strength.	69
Figure 61. Close up of cross-section views from Eiger, TS1-X on the left and TS1-1 on the right.....	70
Figure 62. Cross-section views from Eiger, 3BS1-1 on the top and 3BS1-X on the bottom.	71
Figure 63. Close up from cross-section views from Eiger, 3BS1-1 on the right and 3BS1-X on the left.	72
Figure 64. Tightening tool applications manufactured with Metal X.....	73
Figure 65. Gripper application manufactured with Metal X.	74
Figure 66. Measuring tool application manufactured with Metal X.....	74
Figure 67. Extruded strip from a body, which most likely increase the strength of the part.....	75
Figure 68. Cross section from the part where the strip is extruded. Increased amount of solid material in outer walls is very visible.....	76
Figure 69. Infill settings from Eiger.....	76
Table 1. Tested samples and their dimensions in tensile strength test.....	54
Table 2. Test samples and their dimensions in 3-point bending strength test.	58
Table 3. Test samples and their dimensions in compression strength test.	63
Table 4. The difference in bending direction.....	71

GLOSSARY

3D	Three-dimensional
ABS	(Acrylonitrile butadiene styrene) Common thermoplastic polymer
ADAM	Atomic Diffusion Additive Manufacturing, Markforged Metal X methods name
Alpha test	Acceptance testing, done before releasing the feature, can be done by the potential users or customers
AM	Additive manufacturing known as 3D printing also is manufacturing method where object is built layer by layer.
ASTM	American Society for Testing and Materials, international standardization society
BJ	Binder Jetting, an Additive Manufacturing method
BMD	Bound Metal Deposition, similar method from Desktop Metals as Markforged Metal X
CAD	Computer aided design
CES	The Global Stage for Innovation
CFF	Continuous Fiber Fabrication, Markforged coined term for their FFF process
CNC	Computer numerical control
DCV	Delivery Centre Vaasa, W20, W31, W32 and W34 engines are built and delivered to the customer at DCV.
DED	Direct Energy Deposition
DfAM	Design for Additive Manufacturing

DMLS	Direct Metal Laser Sintering
FDM	Fused Deposition Modeling also known as FFF
FEM	Finite Element Method
FDMet	Fused Deposition of Metals
FFF	Fused Filament Fabrication also known as FDM
G-Code	Numerical control programming language, used in computer aided manufacturing
GPa	Gigapascal, a unit of pressure equals to 10^9 Pascals
HRC	Hardness, measured by the Rockwell scale
HSE	Health, Safety and Environment
ISO	International Organization for Standardization
kN	Kilonewton, a unit of force which equals to 10^3 Newtons
MAM	Metal Additive Manufacturing
ME	Material Extrusion
Micron	Micrometre, one millionth of a meter, equalling $1 * 10^{-6}$ m
MIM	Metal Injection Molding
MPa	Megapascal, a unit of pressure which equal to 10^6 Pascals
Newton	Force needed to accelerate one kilogram to one meter per second squared to the direction of applied force $[\frac{kg*m}{s^2}]$
NPI	New Product Introduction.

Onyx	Markforged Mark Two printer material nylon blended with chopped carbon-fiber
Pa	Pascal, it is a pressure which is caused by one Newton to one square meter of surface [$\frac{N}{m^2}$]
PBF	Powder Bed Fusion
PH	Precipitation Hardening
PLA	Poly lactide, biodegradable thermoplastic aliphatic polyester made from renewable raw materials
Polyolefins	Type of polymers produced from a simple olefin
R&D	Research and Development
STH	Smart Technology Hub, Wärtsilä's new research, development and production center in Vaasa.
STL	Standard Triangle Language or Standard Tessellation Language, describes only the surface geometry of a three-dimensional object
VH10	Vickers Hardness tester
W20	Wärtsilä engine model where number after W is the diameter of the piston in centimetres.

1 INTRODUCTION

This thesis was done for Wärtsilä New Product Introduction (NPI) & Smart Manufacturing department. The purpose of this thesis was to do experimental strength tests with Metal X manufactured specimens. The purpose was to find out the strength of basic geometry, and how much changes in dimensions affect the strength of the specimen.

Three different experimental tests were done: tensile strength test, three-point bend strength test and compression strength test. From every test, multiple different dimensions were examined. Siemens NX was used to create 3D models from the test samples and Markforged Eiger to print and investigate the infill structure. The main point in this thesis was to find out the basic strength of the basic geometries.

The AM is slowly gaining ground in Wärtsilä. New applications for AM are found weekly, and designers in Wärtsilä are starting to gain the knowledge of AM, of course, there is resistance toward new techniques, but it is gaining ground as one manufacturing technique, among others. The main problem with the end-use application for engines is the size of engine parts, which are quite large and the benefits from AM are not so clear.

2 WÄRTSILÄ OYJ

Wärtsilä operates in international market in marine and energy sector, Wärtsilä portfolio includes integrated solutions, global services and innovative products. Wärtsilä is a global leader in entire lifecycle solutions and smart technologies. Wärtsilä net sales in the year 2018 were 5,174 million Euros and a comparable operating result of 577 million Euros. The personnel at the end of the year 2018 was 19 294 globally, from that 20 percent in Finland. Wärtsilä has over 200 offices over 80 countries, in Finland offices are in Vaasa, Turku, and Helsinki. /1/.

2.1 From History to Today

Wärtsilä was established in 1834 in Tohmajärvi. First, Wärtsilä was a sawmill, and in 1908 it became a modern smelting plant and steel mill. Wärtsilä diesel engine era began in 1938 when Wärtsilä started producing diesel engines with a license agreement with Friedrich Krupp Germania Werft AG. Since then, most of Wärtsilä operations have been associated with the metal industry and especially to the marine and power industry. In 2017, Wärtsilä published its vision of smart marine and smart energy. As a result, Wärtsilä will build a new centre, Wärtsilä Smart Technology Hub, in Vaskiluoto, Vaasa (Figure 1). The new Hub is one step closer to the vision of smart marine and smart energy. /2, 3/.



Figure 1. Smart Technology Hub. /3/.

2.2 Organization and Strategy

Today Wärtsilä is divided into two divisions, Energy Business and Marine Business. This organization change was made in January of 2019. Before the organization change, Wärtsilä Service was individual division, but now it is embedded in the Energy and Marine business. In the year 2018 Service was the biggest with 47 percent of the net sale (Figure 2). Wärtsilä's strategies for Energy and Marine businesses are smart energy and smart marine. Smart energy is a strategy to create a path toward 100% renewable energy, and smart marine is for leading societies to smart technologies (

Figure 3). /4/.

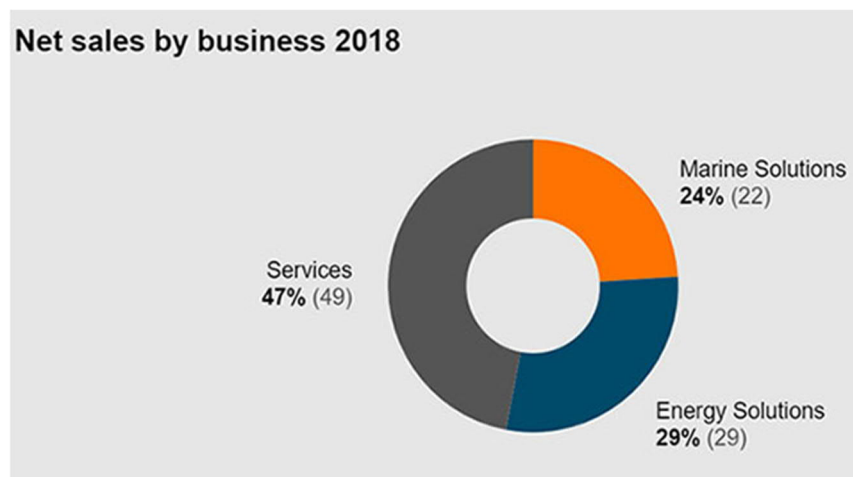


Figure 2. Wärtsilä's net sales by business in 2018. /4/.

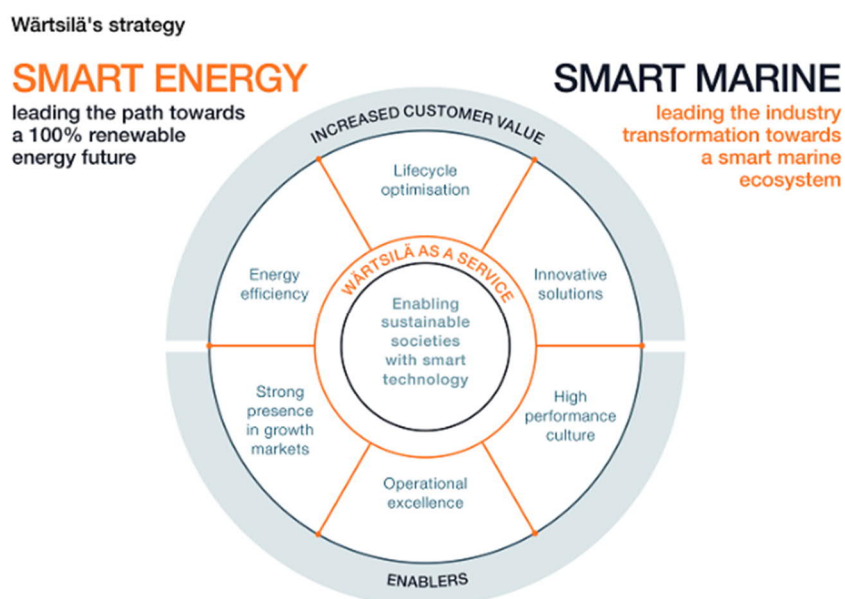


Figure 3. Wärtsilä's strategy. /4/.

2.2.1 Wärtsilä Marine Business

In Wärtsilä Marine Business includes engines from small Wärtsilä 14 with nominal power 54 kW per cylinder to large Wärtsilä 50DF 975 kW per cylinder. They also provide many other applications, such as Exhaust Gas Cleaning systems, Fleet Operations Solutions, Fresh Water Generation, Gas Solutions, Propulsors, and Gears and even Wärtsilä Vacuum Toilets. Wärtsilä offers complete solutions in the marine and energy systems for lifecycle. Wärtsilä engines have proven reliability, low emissions, low operating costs, and fuel flexibility. Wärtsilä Marine Business has a vision of Smart Marine Ecosystem, and Wärtsilä wants to be the leader in the industry transformation. The base for Wärtsilä Smart Marine Vision is to eliminate three major inefficiencies in the marine industry: overcapacity, waiting times and deficient port-to-port fuel efficiency. /5/.

Delivery Centre Vaasa (DCV) is included in Wärtsilä's Marine Business and the main products engines range from W20 to W34 including Wärtsilä's new W31. DCV consists of two- engine assembly unit: pilot factory, line factory, different subassembly units and three engine test facilities for W31, W32, and W34 and one assembly unit for W20 engines.

2.2.2 Wärtsilä Energy Business

Wärtsilä Energy Business offers Power plants from 1 MW to over 500 MW with fuel options of liquid fuel, natural gas or both. The operating profile can be chosen from flexible baseload, intermediate load, peaking, and grid stability or emergency. In the future, Wärtsilä Energy Business will concentrate on a 100 percent pure, renewable energy. With Wärtsilä engine-based solutions, it is possible to have flexible power plants. These include, for example, liquid gas systems where the fuel is liquefied gas instead of gasified liquid gas, or hybrid solar power plants where Wärtsilä engines produce electricity in sunless times. Wärtsilä Energy Business also offers energy management, integration, and storage systems. Energy business will offer its customers support through the lifecycle of Wärtsilä installations. Nowadays Wärtsilä Energy Business has 70 Giga Watt capacities of power in 177 countries all over the world, and it is growing. /6/.

The vision of the new research, development and production facility STH is to create a flexible partner campus. In STH, research and production development are done side by side with Wärtsilä's customers, suppliers and universities. STH will provide a smarter, more agile production and research facility /3/.

3 METAL ADDITIVE MANUFACTURING

Additive manufacturing (AM), especially Metal Additive Manufacturing (MAM), is a new generation of a manufacturing method where material is added instead of removing it. It has grown just in 30 years from decentralized inventor thoughts into a fully developed industry. With AM, it is possible to make shapes and figures that cannot be obtained with any other manufacturing method. AM does not remove the need for traditional manufacturing methods, however it will provide a good option alongside traditional methods. The production of the large series is still usually profitable with traditional manufacturing methods, unless Additive Manufacturing imports something unique to the design. /7/.

The sales of Additive Manufacturing system has increased rapidly in the 21th century, from the year 2000 to 2010 there has been a steady rise, but after 2010 the rise has been exponential. In March 2019 177 manufacturers sold industrial-grade AM machines with a value of 5000 \$ or more. 27 manufacturers sold more than 100 machines (Figure 4). These numbers include all Additive Manufacturing methods, plastic and metal. /7/. The numbers demonstrate that AM is gaining the ground as a manufacturing method, and it is not anymore just for rapid prototyping.

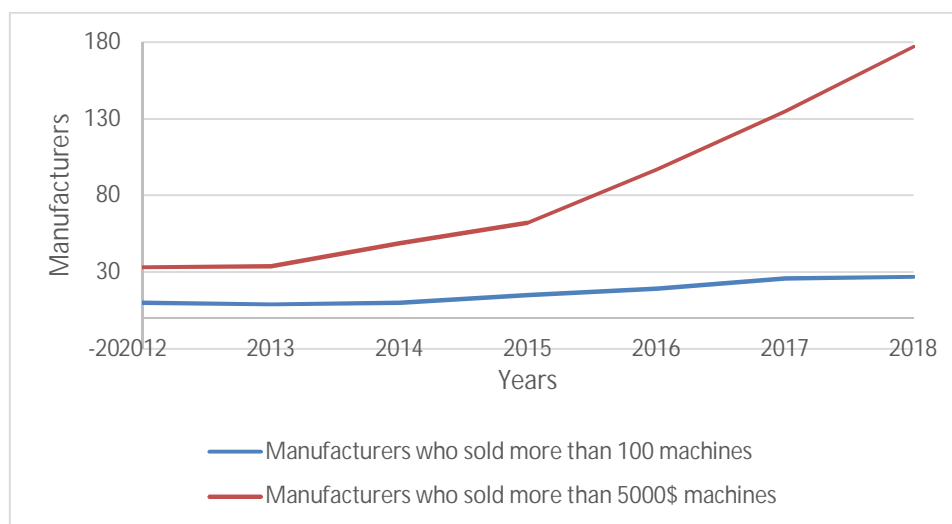


Figure 4. The increase of AM machine manufacturers from 2012 to 2018. /7/.

3.1 Characteristics of Metal Additive Manufacturing

Additive Manufacturing consists of different technologies, which differ from each other by materials and methods. Methodologically AM is divided into seven different groups by ISO/ASTM DIS 52900, five of them, are used in Metal Additive Manufacturing. Powder Bed Fusion (PBF) is a good method to achieve parts with high strength and complex geometry, however the size and the price of the parts are still an issue in many cases. Binder Jetting (BJ) manufactured parts does not have the strength of PBF parts but it is a much faster method, however the design freedom is not as good as in PBF. These two methods are the most used methods in Metal Additive Manufacturing. Followed by Metal Extrusion (ME), which is the Markforged Metal X principle and it is a very good method to be familiarized with MAM. Other methods used in MAM are Direct Energy Deposition (DED), which is the fastest method of AM and it can be utilized in large obstacles, however it is the most rough method of AM. /7, 8/.

3.1.1 Powder Bed Fusion

Powder Bed Fusion (PBF) is the most used method for 3D printing metals. PBF offers excellent design freedom with good material properties. It is a method where a layer, usually from 20 μm to over 50 μm of powder is spread to the build platform by a recoater. The laser or electron beam melts the cross-section of the geometry (Figure 5). After the powder is melted, the build platform lowers down the thickness of one layer, and a new layer of powder is spread to the build platform (Figure 6). /9, 10/.

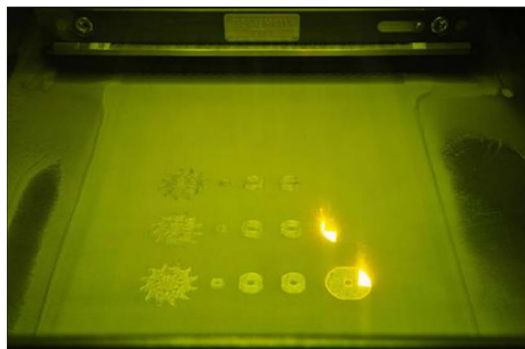


Figure 5. A picture showing Renishaw's PBF print process in action. /9/.

The process of melting, lowering the platform and recoating is continued until the part is completed. PBF processes include different kind of terms and every manufacturer has their own term for their process, for example Selective Laser Sintering (SLS) and Selective Laser Melting (SLM). However all the terms in that category are practically the same, slight differences for example in heat sources but the principle is more or less the same /9, 10/.

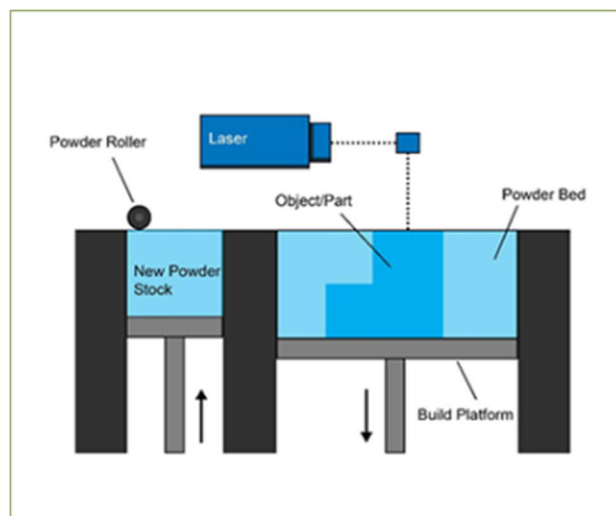


Figure 6. The principle of Powder Bed Fusion. /9/.

There are multiple compulsory steps after the printing job is completed. Since the parts are usually welded onto the build platform, it needs stress-relieving in an oven to prevent deformations which can be formed due to the welding process. The removal of the build job and the supports from the print bed, usually this is done with a bandsaw or with electrical discharge machine. Supports are usually always necessary to keep the build job contacting the build plate (Figure 7), and for transferring the heat from the part to the build plate. However, support-free is plausible in some special cases and there have been manufacturers who claim that supports are not needed anymore in their methods but that is still under investigation. After those steps are taken, the part usually needs in some extent CNC machining, especially

for the features requiring high dimensional accuracy, heat treatment or Hot Isostatic Pressing, and smoothing or polishing. /11/.**Figure 7**



Figure 7. A metal bracket before supports are removed. /11/.

The recoater and the thermal deflections together are causing the biggest issues in PBF. If the thermal deflections due to the welding process are big enough, it may lead to deformations in the part and therefore to contact with the recoater, which spreads the powder just above micrometres. Mainly because of the recoater, the part needs to be attached to the build platform by support structures, which are removed afterwards, and this increases the manual labour time. However, companies are developing machines to prevent these issues, for example Velo 3D, where the recoater is a non-contact, thus, the recoater has no contacting point to the built part in any cases. The melt pool control system is a closed loop, therefore it will adapt for example the laser power based on the scanner heat results and therefore no part needs any support structures. It is a great improvement compared to current PBF methods.

However, Velo3D has not revealed the mechanism behind the non-contact recoater, but the results look promising (Figure 8). /12/.

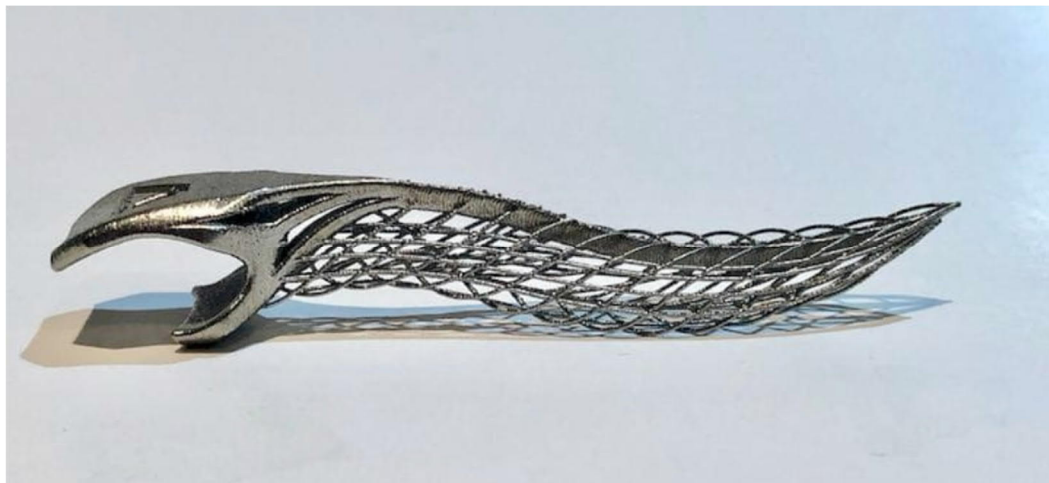


Figure 8. Support free bottle opener manufactured with Velo3D. /12/.

3.1.2 Binder Jetting

In Binder Jetting (BJ), the metal material is the same as in PBF only finer, but the material mixture is based on Metal Injection Molding (MIM) technology. A layer of metal powder, typically 50 μm , is spread on the build platform, inkjet nozzles selectively deposits drops of a binder, which is a polymer and a wax, according to the sliced 3D-model (Figure 9). The binder bonds the metal powder particles and forms a solid but fragile metal part. After the part is printed, it is a “green part”, which needs to be washed to a “brown part” and subsequently sintered or infiltrated to a dense metal part. Compared to other metal additive manufacturing technologies, binder jetting does not need any support structures during the building phase, however, they are still needed in the sintering phase. BJ has a relatively large building chamber compared to PBF, therefore BJ is suitable for low-to-medium batch production. The mechanical properties are not as good as with PBF, since the sintering phase leaves approximately 3 percent porosity to the part. That is why high-end applications are not suitable to manufacture with BJ due to the dynamic stress /13/.

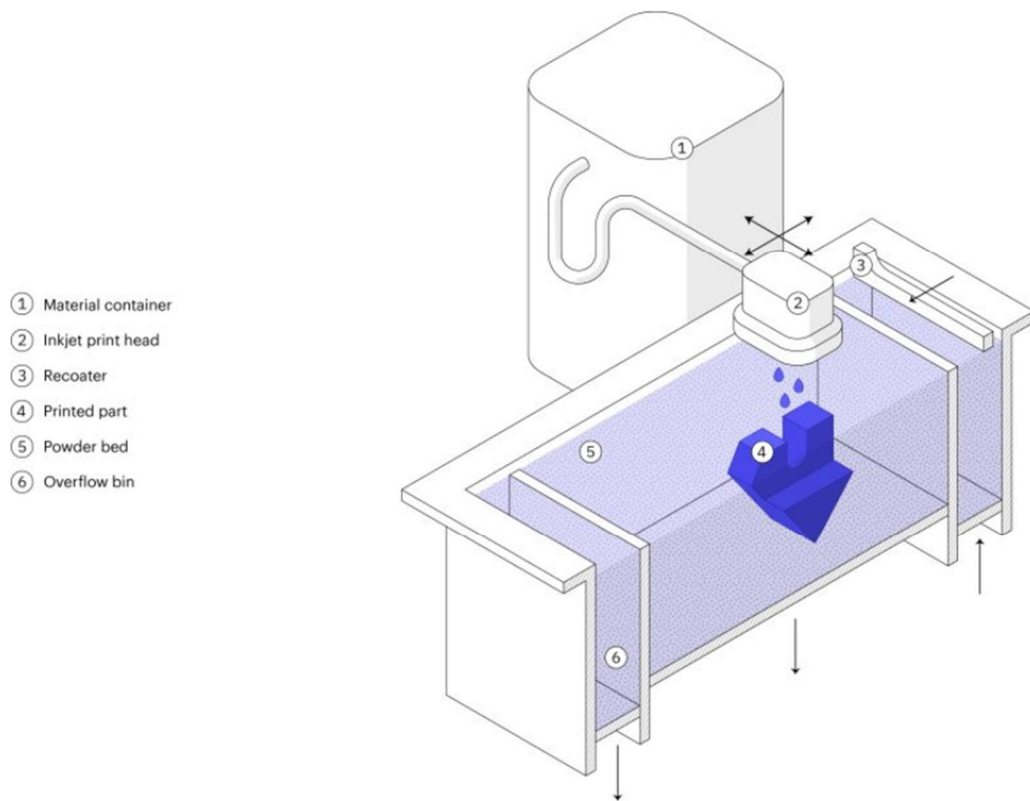


Figure 9. Binder Jetting printing process. /13/.

3.1.3 Direct Energy Deposition

Direct Energy deposition (DED) is a basically a robotized welding, and the heat source is a laser, electron beam or plasma arc. The material is added in form of powder or wire, it is spread through a nozzle and the heat source melts the added material to the base material according the sliced 3D-model (Figure 10). In DED the base material can be almost any shape due to the programmable robot, which is not possible with any other AM-technique /14/.

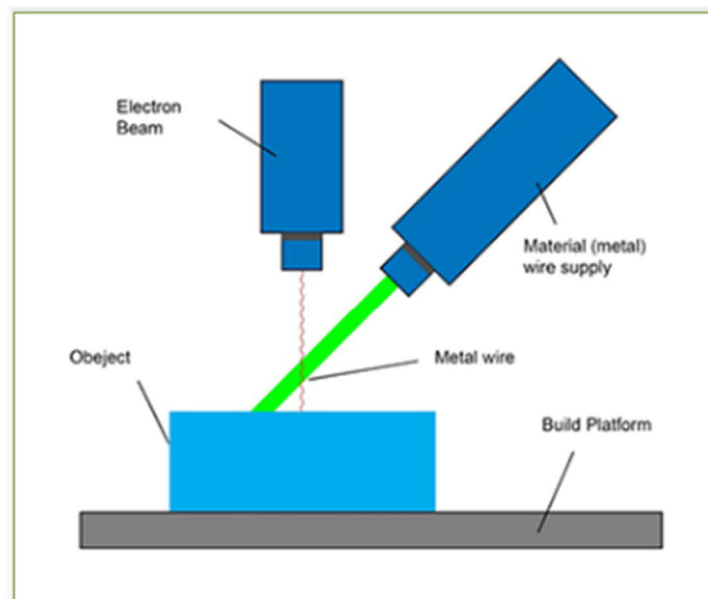


Figure 10. The principle of Direct Energy Deposition. /14/.

In DED processes as in PBF, different methods are numerous, for example Laser Metal Deposition (LMD), Wire Arc AM (WAAM) and so on. All methods in DED category are basically the same, heat source or added material variates.

When comparing DED and PBF, they both have their places in the field of additive manufacturing. DED is much faster than PBF, but the PBF is on the other hand much more precise, therefore, DED is best in applications where the part will be machined afterwards. DED has much larger manufacturing capability than with PBF. The size of the component to be built is limited in DED by the robot trajectories and in PBF the process chamber, which varies from a small 8 dm³ to a large 160 dm³ chambers. Part complexity is limited with DED but nearly unlimited with PBF. /14, 15/.

3.1.4 Metal Extrusion

Metal extrusion (ME) is method where material is extruded through the nozzle, layer by layer, according to the 3D-model (Figure 11). Extrusion methods are usually connected to plastic printing, major part from extrusion-based printers are plas-

tic. After Markforged published their Metal X machine, at the Global Stage for Innovation (CES) 2017, extrusion cannot be thought anymore just plastic printing method. /16/.

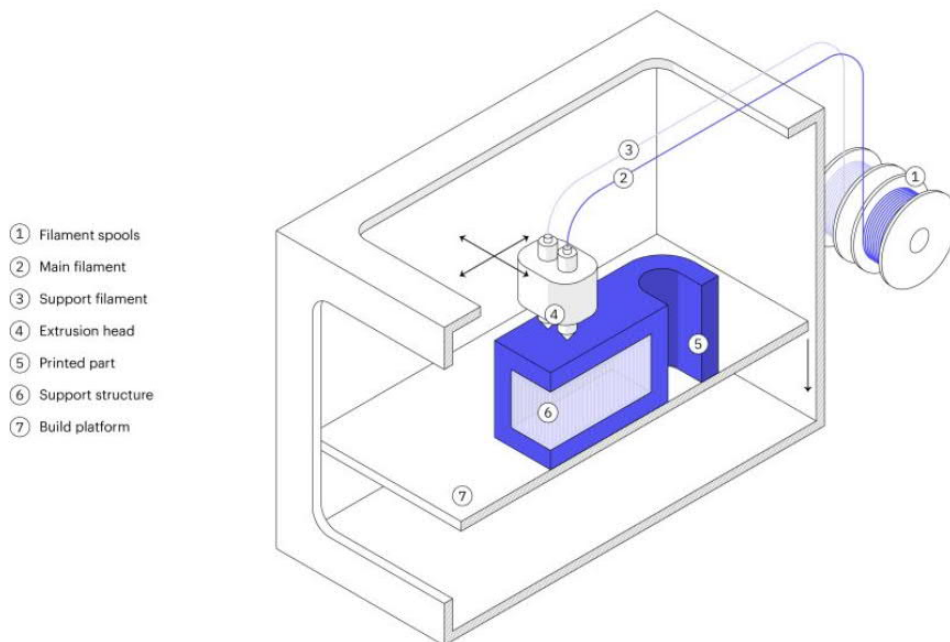


Figure 11. The principle of Metal extrusion. /13/.

The FDM -based Metal Extrusion is also known by the names Bound Metal Deposition (BMD) or Atomic Diffusion Additive Manufacturing (ADAM). Unlike plastic extrusion printing, the part is not ready from the printer. It needs to be washed and sintered, as in Binder Jetting. The material in ME comes in the form of a spool or a rod, and it is usually a compound of metal, polymer, and wax. Unlike with many other MAM processes, with ME, parts can be printed as hollow, with an infill. Support structures are needed, exactly as in a plastic FDM printer. Even though the metal material is powder, just like in Powder Bed Fusion, because it is bonded with polymer and wax, it is much safer to use than in Powder Bed Fusion. /17-19/.

Every method above has its own place in the field of AM. Choosing the correct manufacturing method for applications is important, for example ME is a good

method for parts, which have low volume and low complexity, PBF on the other hand is a perfect method for parts high complexity and low volume (Figure 12).

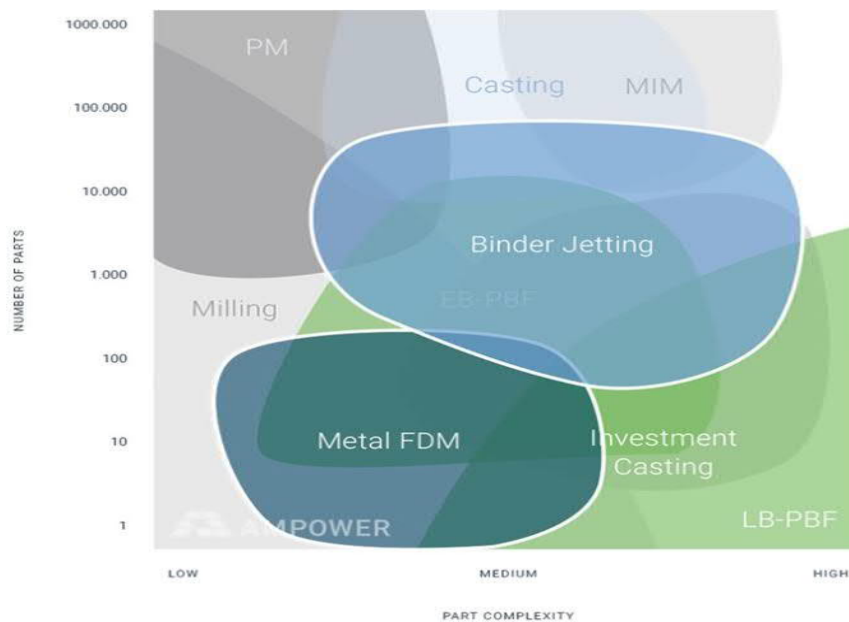


Figure 12. Comparison between metal manufacturing techniques. As it can be seen, every AM method is located where the batch size is smaller, but the complexity of the part is higher /20/.

3.2 Value of Metal Additive Manufacturing in industry

The possibilities with AM are enormous, a few years back it was impossible to dream of objects, which can be manufactured today /21/. Additive manufacturing is often characterized as a process which is capable of building geometry of any kind, however this is somewhat biased. With AM, greater design freedom is provided compared to traditional manufacturing, but it has its own constraints. To unlock the value from AM all the constraints and peculiarities should be carefully considered and studied. /22/.

3.2.1 Improved Performance through Design

Additive manufacturing might offer improved performance, for example with targeted cooling capabilities and product designs which traditional manufacturing

methods cannot achieve, for example, lattices, hollow structures, and complex shapes. Lattice and hollow structures could be utilized for example in heat exchangers to manufacture optimized flow channels and light structure. Complex tools, casts or forgings, which are needed in traditional manufacturing, are no longer needed in some applications made with AM, which could save time and money (Figure 13 & Figure 14). /23/.

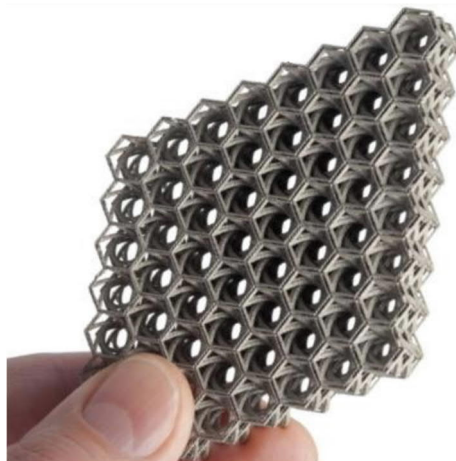


Figure 13. Lattice structure manufactured with PBF. Creating the lattice structure inside the part could help to minimize the weight while retaining the strength.

/24/.

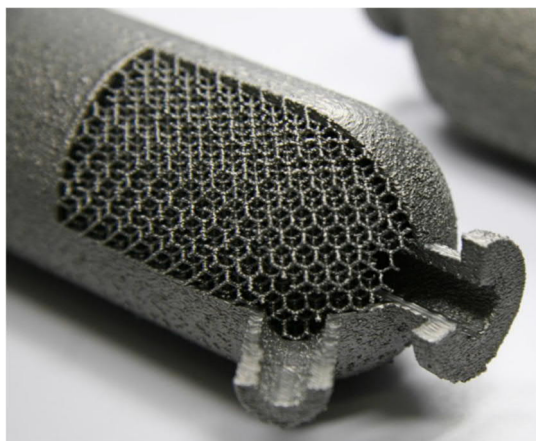


Figure 14. Lattice structure manufactured inside the chamber by PBF. For example, heat exchangers with optimized geometry for flow rate could gain benefit

from this. /24/.

3.2.2 Possibilities of AM

Components, which are traditionally assembled of multiple parts, can be manufactured as one with AM. A great example of this approach is General Electric's fuel nozzle. Earlier it was assembled from 20 different parts, and today with AM it can be manufactured as one, thereby saving in weight 25 %. Part strength, on the other hand, is improved by a factor of five compared to the original one (Figure 15).

/25/.



Figure 15. General Electric's fuel nozzle, where 20 different part has been consolidated into one with AM. /26/.

The key question for companies gaining the value from AM and to utilize AM is different, depending on what kind of value they are looking for. Different value drivers may be related for example to efficiency, performance, time, flow optimization, integration of functions, mass customization, shortening lead-time, or automated manufacturing (Figure 16). /24/. The most challenging issue is to identify the parts, which could benefit from AM, there is no direct answer or software for that.

Design offices have developed their own programs, to identify parts suitable for AM but these programs are always indicative and may give results based on the part volume, yearly volume and simple complexity but the responsibility lies with the designer and with his experience /23/.

		VALUE DRIVERS		
		Performance	Time	Production Cost
APPLICATIONS	Prototyping <i>for product development</i>	✓	✓	
	Spare Parts <i>for service</i>		✓	✓
	Fixtures <i>rapidly print manufacturing aids</i>		✓	
	Assembly Consolidation <i>reduce assembly costs and improve performance</i>	✓		✓
	Lightweighting <i>remove mass with geometry not possible conventionally</i>	✓		
	Conformally Cooled Tooling <i>improve molding/casting cycle time and part quality</i>	✓	✓	✓
	CNC Machined Parts <i>printing near-net-shape to reduce scrap and machine time</i>		✓	✓
	Low Volume Previously Cast Part <i>eliminate tooling to reduce lead time and cost</i>		✓	✓
	Low Volume Previously Forged Part <i>eliminate tooling to reduce lead time and cost</i>		✓	✓
	Low Volume Previously Stamped Part <i>eliminate tooling to reduce lead time and cost</i>		✓	✓
	Multi-metal <i>producing new part designs that combine multiple metals</i>	✓		

Figure 16. Different applications and their value drivers. /23/.

Design for Additive Manufacturing (DfAM) is the key for succeeding and gaining the value from AM. Topologically optimized structures, better strength-to-weight ratio, lattice structures to reduce material consumption and weight, conformal cooling channels are all results of DfAM. Because industries start to utilize Additive Manufacturing in every area, the need for better software and qualified workforce is increasing. Software companies are constantly developing software and publishing updates for designers to help them succeed in DfAM. Universities and educational institutes have also taken AM as a part of their educational program, to achieve more AM skilled labour in the future /7/.

Mass customization is one great advantage of AM. With traditional manufacturing, mass customization has been expensive because every minor change in the final

product causes extra work in the manufacturing phase and therefore extra cost. With Additive Manufacturing the only change is made in 3D model, therefore there are no extra costs in the manufacturing phase. With customized products, individual parts can be produced for customers. Many examples can be found, for example, hip or dental implants where implants are manufactured specifically for the customer. The car manufacturer BWM has made a customization package for MINI where their customers can customize different parts from their car, for example, LED door sills, dashboard and side scuttles. /7/.

3.3 The Future of Additive Manufacturing

Materials diversification will become more important in the future. New materials are developed and published to the market every year. One important trend will also be fine-tuning, especially their processing-property relationship, of materials already existing, such as Ti-6Al-4V and Inconel /7/.

Design for Additive Manufacturing is coming more standardized in the future, now there are 28 different ISO/ASTM standards published or in stage of development for Additive manufacturing. The first DfAM standard was published in July of 2019. This standard will provide design recommendations for designing to Laser powder bed fusion, another one was published in August of 2019. /27/.

More and more focus will be on post-processing of manufactured parts because the time and money spend on post-processing is not productive. The post-process includes, among other things, support structure removal, which often is manual labor, also stress relief, heat treatments, finishing, and packing is post-processing. Post-processing may cost as much as the AM build itself, therefore planning all the needed post-processing steps during the design phase is crucial. Manufacturers are developing their machines to be more independent, such as rotating and vibrating powder removal systems, which will assist the AM process chain (Figure 17) and support material removal through the electrochemical wash, which will affect the part itself relatively little. /7/.

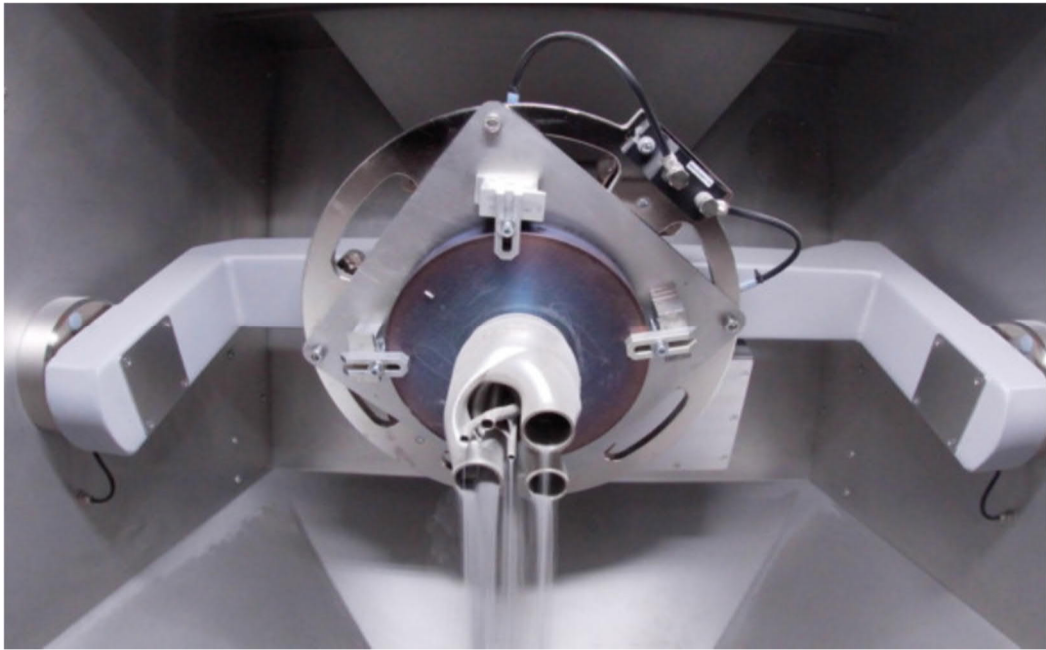


Figure 17. Solukon powder removal machine. /55/.

3.4 Additive Manufacturing in Wärtsilä

Additive manufacturing era in Wärtsilä started in the year 2009 with the Wärtsilä W31 engine industrialization project. AM was thought to be used for visualizing different concepts and for example Turbocharger, Power-pack, and Crankshaft sub-assemblies for W31 engine. In 2014 Wärtsilä did first studies with Metal Additive Manufacturing, the result was not a success, however, it was due to the lack of AM understanding that time. Within the last two years, Wärtsilä has been investigating MAM and the benefits from it and studying the AM in general not to make the same mistakes.

The idea for Wärtsilä's first 3D-printer in 2009 came from the head of NPI & Smart Manufacturing of that time, from Switzerland and Wärtsilä did a feasibility study of Direct Manufacturing in September 2011 based on that idea. Based on that study, Wärtsilä bought a Fortus 400mc, which is and was a good extrusion-based plastic printer (Figure 18).



Figure 18. Fortus 400mc. (Feasibility study for Wärtsilä.)

Fortus 400 was chosen because it was possible to manufacture large parts and because the support material needed only ultrasonic wash for postwork. Fortus 400 was the only AM machine in Wärtsilä for years, in early 2018 came second plastic printer, which was Ultimaker S5 and the third printer which was Markforged Mark Two, composite printer, at the end of 2018. Now Wärtsilä manufactures a different kind of tools and help equipment with Additive Manufacturing. There still are no end-product parts manufactured with AM, but the first steps are already taken toward that, what kind of parts are possible and useful to manufacture with AM. The decision for Metal X in September 2018 was based on Juho Raukola's Master's Thesis, Characteristics of Metal Additive Manufacturing in Four-Stroke Engine Manufacturing Process, 2017. Metal X was bought for manufacturing visualization models and tools from metal at the factory.

4 METAL FUSED DEPOSITION MODELING

The company Markforged was founded in 2013 by an MIT aerospace engineer Greg Mark. Their first printer Mark One was a composite printer, after they released Mark Two, which could print continuous Fiber inside the part. These printers have been the foundation for their metal printer Metal X. /29/. The Metal X is Markforged first metal printer and is the world's first Atomic Diffusion Additive Manufacturing machine. /30/.

In the year 2018 Markforged shipped 100 units of Metal X just in 6 months representing almost ten percent in Metal Additive Machine markets and top distributor in Sintering machines. /31/. Markforged recent public evaluation is from November 2017 when it was evaluated as \$300 million. For 2018 Markforged revenue forecast was \$70 million but Markforged did not reveal the specific revenue, or new evaluation. /33/.

4.1 Metal X

Metal X is a complete system, which includes a printer, a washer, and a sintering oven (Figure 19). Metal X's method ADAM, is based on Fused Deposition Modeling (FDM), and in Metal Injection Moulding. It is a cost-effective, and unique AM method, now there is only one other machine with the same method, except that method is called, Bound Metal Deposition. These machines suit very well to produce small series and prototyping because of their build size 250mm x 220mm x 200mm is smaller than many other MAM machines and because the need for machine environment is not as critical as, for example, in PBF. /27/. Strataysys was the first to introduce the idea of fused deposition of metals (FDMet) in the 90s. /34/.



Figure 19. Metal X entity. /30/.

4.1.1 Materials

There are six different metal materials available for Metal X now:

- 17-4 PH Stainless Steel
- H13 Tool Steel
- A2 Tool Steel
- D2 Tool Steel
- Inconel 625
- Copper

Other metals such as 316L and Titanium 6-4 are on the way, but still on the beta test phase. /27/. Within this thesis, 17-4 PH Stainless Steel is examined. It is most widely used stainless steel and is used in all types of industries such as aerospace, chemical, paper and metal industries. /35/. It has Ultimate Tensile Strength 1050 MPa as sintered, tensile modulus 140 GPa and hardness 30 HRC /36/. The metal

powder in Metal X material is the same as they use in Powder Bed Fusion processes except it is combined with plastic and wax like in MIM. /37/.

4.1.2 Print Preparation

All Markforged printers are handled from Eiger, cloud-based slicing software (Figure 20). After a 3D-model is finished in the CAD software, it will be converted into the STL format and imported into Eiger. After importing the model, a designer will choose a material, a printer, an orientation and choose the part and the material settings. Eiger is designed to handle multiple Markforged printers in one software. After designer has chosen the correct parameters, Eiger will slice the STL file into a G-code. The G-code is a computer language for computerized machine tools, based on the created G-code, the printer will build the part layer by layer.

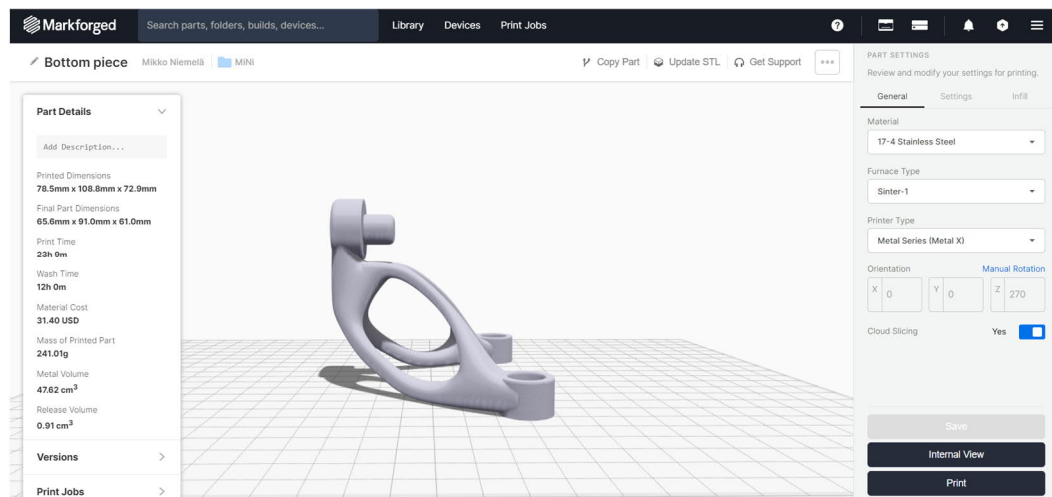


Figure 20. Part view page from Eiger, part detail information is on the left, and part settings information is on the right.

After sliced the 3D-model, Eiger will show part details, for example, final part dimensions, print time, estimated wash time and material cost based on selected material (Figure 21).

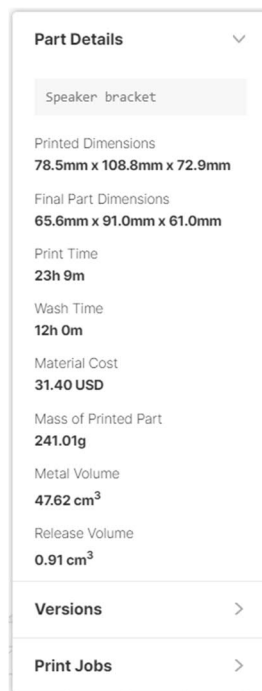


Figure 21. Part detail window in Eiger.

From the printing settings the printer is selected or choose to export the build to a hard drive. From there it can also be selected which parts will be printed on the same print, and how the parts are orientated on the print sheet. The Internal View page helps designer to inspect, for example, the support material placement and the layer –by- layer view helps to understand if there is some design point which needs to be changed (Figure 22).

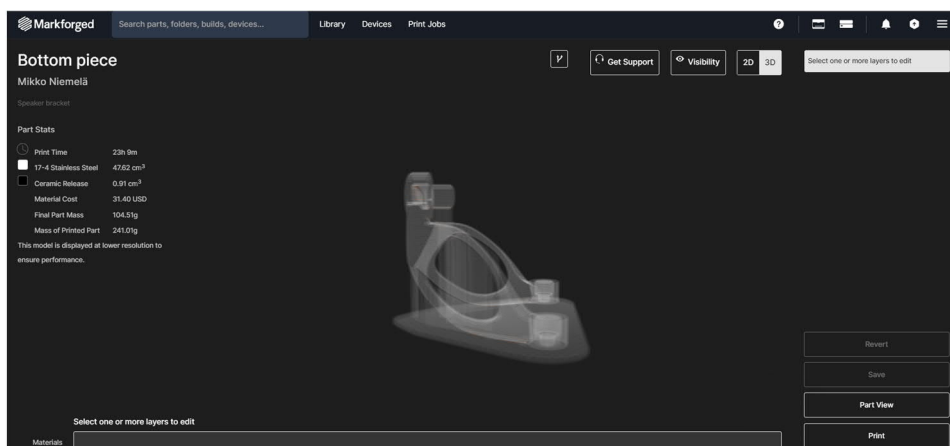


Figure 22. Internal View page, where it can be seen layer by layer how the part will be printed, where support materials, ceramics and materials are printed.

4.1.3 Print Process

The Metal X print process is based on Markforged composite printers and their techniques. /38/. Metal X is like a regular FFF printer, the material is stored in a spool, and it is spread through the heated nozzle to the build platform. The material is a mixture of three ingredients: metal powder, plastic backbone, and the soluble binder. Material is similar as in Metal Injection Molding, the backbone is usually elastomers or amorphous polyolefins and the soluble binder is wax. The backbone in the material is for holding the metal particles in shape until it is sintered, and the wax is for improved viscosity in the printing phase. /34/. Metal X includes two nozzles, one is for metal, and the other is for the release material, which is ceramic, plastic, and wax. The ceramic layer is spread between the part and the raft or the support material, which turns into dust in the sinter, and eases the removal of the part (Figure 23).



Figure 23. The white ceramic release layer, which makes the part release from the raft easier.

The printed part is called a “green part”, and it is metal particles bound with plastic and wax. After the print, the “green part” must be washed in a special fluid, which will solvent the wax of the part. There are two options for wash fluid, Opteon Sion SF-79, and Tergo Metal Cleaning Fluid. Both fluids are designed to clean hydrocarbons, silicones and waxes /39, 40/. It is very important to wash the parts before sintering; if the parts are not washed properly, it can clog the filters, exhaust piping and fittings in the furnace. The whole furnace will need to be cleaned and filters changed prematurely. The wax that has not been washed off can melt and destroy the part, slumping, cracking, fully melted and destroyed parts are all possible results. If there are other parts in the furnace at the same time, they may or may not survive without issue, however, the chance of clogging and an aborted run greatly increases and suggest that all parts in the run may be damaged or destroyed. /41/.

After the part is washed, it is called a brown part, and it must be sintered before use. The sintering program is three-phase, and it includes the debinding phase before the actual sintering phase. In the debinding phase, the remains of the soluble binder and the plastic backbone will be burned away in milder temperature. After debinding, the actual sintering phase is executed, within that time temperature of the sinter is brought close to the metal material melting point, where the metal atoms are diffused (Figure 24). With 17-4 PH Stainless Steel is the melting point 1404 – 1440 °C. From literature it can be found that the sintering temperature is from 1260 to 1380 °C, depending on what kind of material properties are wanted. The actual sintering temperature in the Metal X Sinter is proprietary, but it is approximately 85 percent from the melting temperature of the material. /29, 34, 35, 42/.

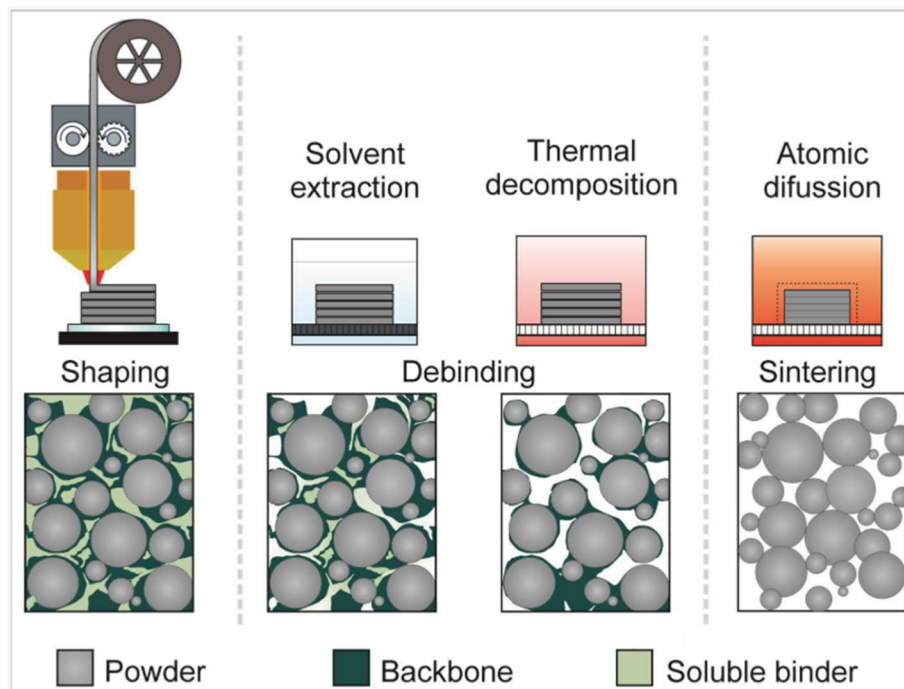


Figure 24. Schematic representation of the shaping, debinding, and sintering process. /42/.

4.2 Pros & Cons

Compared to other MAM machines, Metal X is very fast when it comes to changing printing material. For example, in PBF machines, changing the printing material may take a day because all residues of powder must be removed before changing into another material, which is why it is recommended a machine per material when producing production parts, R&D is another matter. With Metal X, changing the material takes less than half an hour.

Metal X is a very cost-effective MAM method by investment cost, the cheapest PBF machines cost roughly 400 000 US\$, the whole Metal X is available at just under 100 000 US\$. The post work of the parts is relatively simple, compared to PBF, because of the ceramic release layer between the actual part and the support material the part can just be snapped off. Safety when handling materials in Metal X is much better than PBF, even though the metal powder is the same. The metal particles in powder is dangerous if inhaled or handled without safety equipment,

but in Metal X the material is compound of powder, plastic, and wax. Unlike in PBF, the metal powder is not floating freely. /29, 43/.

The process from the 3D-model to the actual part takes more time with Metal X than for example, with Powder Bed Fusion. The printing process itself is slower than in PBF, even though PBF has stress-relieving heat treatments after the printing and the support removal takes longer time but it takes still less time than the wash and the sintering phase in Metal X. The wash phase depends on the geometry and the size of the part, however the minimum of 12 hours. Currently the sintering phase takes 27 hours regardless of the size, or the geometry (Figure 25).

Figure 25. Same part compared with PBF and Metal X, if printed multiple parts the PBF process is clearly much faster.

Sector V02 02	Metal X	PBF
Printing time	26 h	9 h 43 min
Build plate removal	2 min	30 min
Washing	12 h	-
Stress relieving / Sintering	27 h	2 h
Cooling	Included in sintering	2 h
Support removal	10 min	2 h
TOTAL	65 h 12 min	16 h 13 min

Mechanical strength properties in ME produced parts are not as good as in parts produced with PBF. The main reason for the lack of strength in ME parts is the porosity inside the part (Figure 26), and parts made with Metal X have a triangle infill inside the part (Figure 27) while parts manufactured with PBF are solid unless otherwise designed. It is the infill inside the part, which makes the part lighter compared to other metal manufacturing methods, but which also makes it weaker. There is an option with Metal X to print the part as solid, but then it would be reasonable to print it with PBF than with ME, or machine it, depending on the geometry.

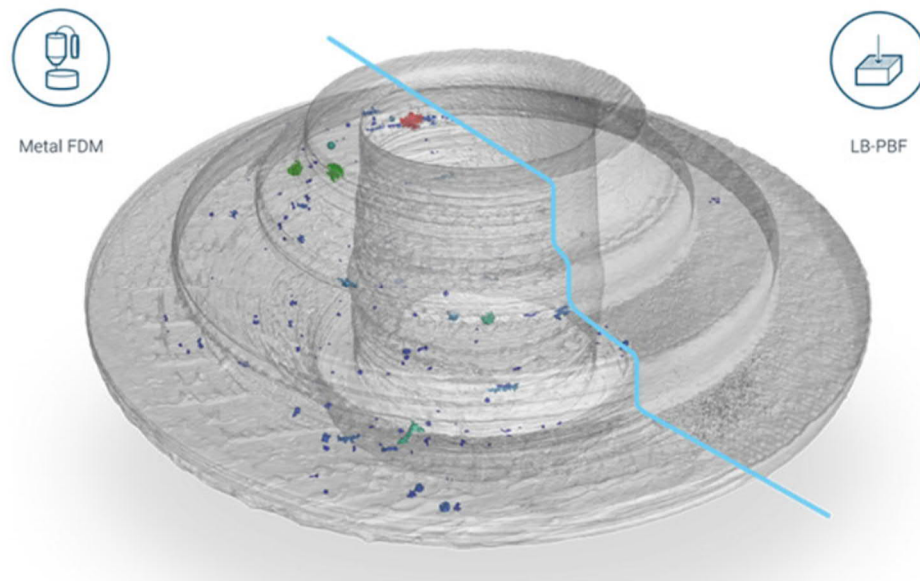


Figure 26. CT analysis of the same part printed with LB-PBF and Metal FDM. The porosity inside the Metal FDM produced part is significant compared to LB-PBF produced part. /20/.

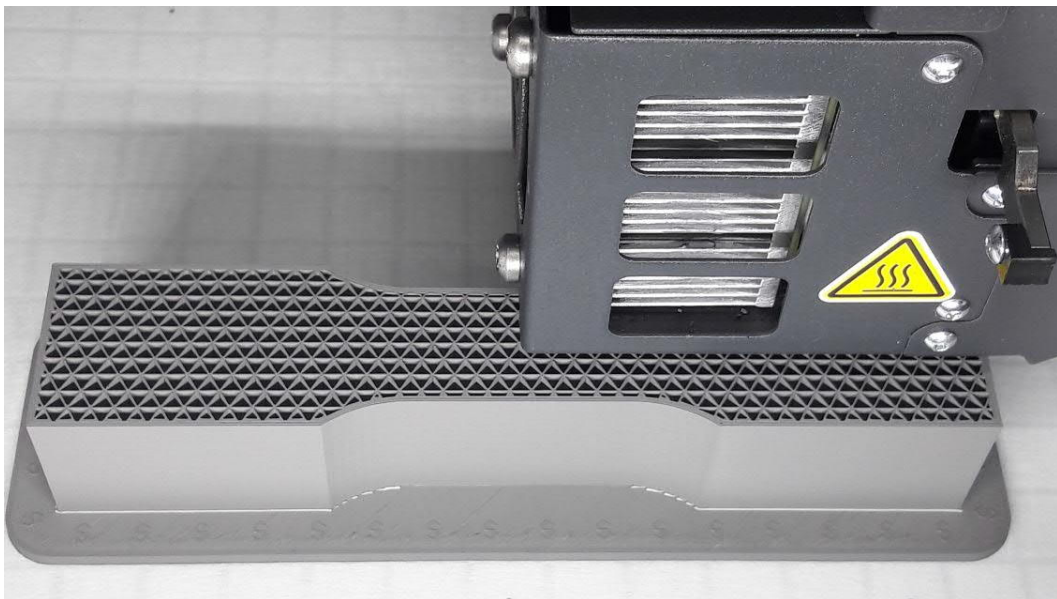


Figure 27. The infill structure in printing phase is well seen.

4.3 Metal X, Commissioning and Factory Assembly

Metal X is a system that comprises printer, washer, and sintering unit. The requirements for the atmosphere for Metal X are not critical, normal room temperature, and humidity are good enough. The ventilation must be arranged for all three, the washer needs ventilation since the fumes from the washing liquid are harmful if inhaled. The sinter needs ventilation since the sintering process takes place using argon, and the exhaust fumes from the process must be led outside the room. For the printer, the ventilation is not obligatory but there may be some thermoplastic fumes from the printing process. /45, 46/.

Two different places were considered for Metal X installation, the first option, building a new room at the factory was ruled out due to the floor vibration during the normal activity at the factory. The furnace oven is sensitive to the vibration because the ceramic furnace tube may be damaged. The second option was a separated production facility inside the factory, which had a suitable environment and enough space for both operations, large pump installation and for Metal X. Sinter needs two different gas for operation, argon, and a mix-gas, which is 2,9 percent of hydrogen and 97,1 percent of argon /45/.

When the decision for purchasing Markforged Metal X was made, the Health, Safety, and Environment (HSE) department were informed. The HSE was included at a very early stage because 3D printing is still quite a new manufacturing method, especially in Wärtsilä, and there are quite a many health factors among many other factors to consider. The discussion with the HSE included gas, washing fluid, fire safety, air conditioning and ventilation, process, and the state.

Finland Institute of Occupational Health has made an instruction for safe 3D printing, where there are basic instructions what to consider when dealing with 3D-printing technology. For example, what printing material is used, if printer is encased, and how to post process 3D-printed parts. /47/. They have also made a model example on how to deal with 3D-printing chemical safety at the workplace, and what to consider when dealing with different kind of 3D-printing technologies, and a

checklist when the company is considering 3D printing from employ and employer view. /48/.

The installation of the system went well, there were no big complications, or problems, only a few misunderstandings with electricity and because of that, more cables had to be drawn. The Metal X system is made easy to use and install. The importer's assembler was with us all the time and kept training for users from the Metal X system. The sinter was the only one that needed something more than plug and play. After the ceramic furnace tube was installed, it had to be combusted and run a calibration run before it could be taken into use (Figure 28).



Figure 28. Pre-combustion run of the sinter before use.

5 MATERIAL TEST EXPERIMENTS

The strength of the material is a study where an object is exposed to stresses and strains. Methods to investigate stresses and strains are many different, but common to all is to try to find the forces the material can withstand without plastic deformations or failure. /49, 50/. The methods used in this thesis are the tensile test, a three-point flexural test and a compression test. These test methods can calculate constants used in simulations and finite element method (FEM) calculations when designing with the same material. It is crucial to know the strength of the material so that designers may design and optimize parts properly.

The tensile test is a method to find out the static strength properties and deformation ability. The test sample is loaded with a steady force that tries to elongate the sample along the axis (Figure 29), usually until failure. With this information it is possible to calculate the strain and the stress of the material, and the Young's modulus which measures the stiffness of the material. /49-51/.

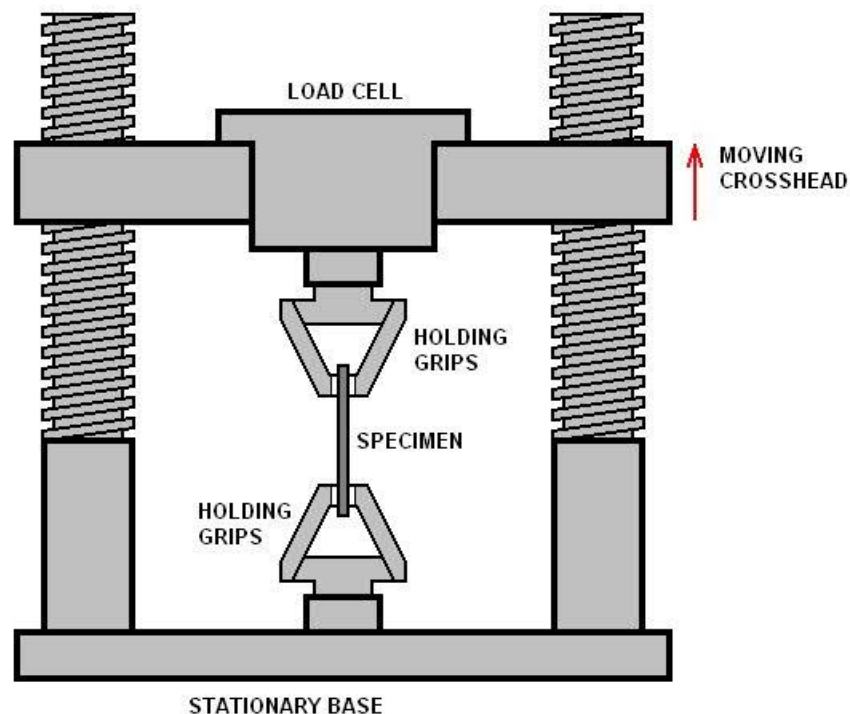


Figure 29. The principle of tensile test machine. /52/.

$$\sigma_t = \frac{F}{A}, \quad \text{where } \sigma_t = \text{Tensile stress}, \quad (1)$$

$F = \text{Force applied},$

$A = \text{Area of the cross – section}$

$$\varepsilon_t = \frac{\Delta L}{L_0}, \quad \text{where } \varepsilon_t = \text{Tensile strain}, \quad (2)$$

$\Delta L = \text{Change of length},$

$L_0 = \text{Initial length}$

$$E_t = \frac{\sigma_t}{\varepsilon_t}, \quad \text{where } E_t = \text{Young's modulus in tensile strength} \quad (3)$$

$\sigma_t = \text{Stress},$

$\varepsilon_t = \text{Strain}$

The three-point bending test is a method where the force is applied to the middle of the test sample, which is laid between supports (Figure 30). This method provides information from the flexural stress, the flexural strain, and the modulus of elasticity in bending. In an ideal material, the modulus of elasticity is the same as Young's modulus, but usually, these values differ from each other, especially with plastics. With the same material, the modulus of elasticity should always be the same regardless of the sample dimensions. /49, 50, 53/.

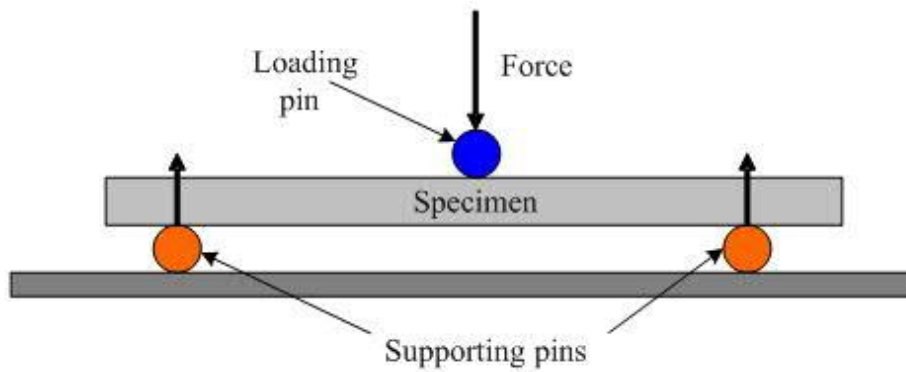


Figure 30. The principle of 3-point bending test. /54/.

$$\sigma_f = \frac{3FL}{2wh^2}, \quad \text{where } \sigma_f = \text{Flexural stress}, \quad (4)$$

$F = \text{Force applied},$

$L = \text{Support span},$

$w = \text{Width of test sample},$

$h = \text{Thickness of test sample}$

$$\epsilon_f = \frac{6Dh}{L^2}, \quad \text{where } \epsilon_f = \text{Flexural strain}, \quad (5)$$

$D = \text{Maximum deflection of the sample},$

$h = \text{Thickness of test sample},$

$L = \text{Support span}$

$$E_f = \frac{L^3 F}{4wh^3d}, \quad \text{where } E_f = \text{Modulus of elasticity}, \quad (6)$$

$L = \text{Support span},$

$F = \text{Load applied}$

$w = \text{Width of test sample},$

$h = \text{Thickness of test sample}$

$d = \text{Deflection of sample}$

A compression test is a method where the test sample is exposed to the forces, which try to compress the test sample along the axis (Figure 31). Usually when testing metal samples with compression test, it is difficult due to isotropic structure and compression strength of the metal being higher than tensile strength. /49, 50, 53/.

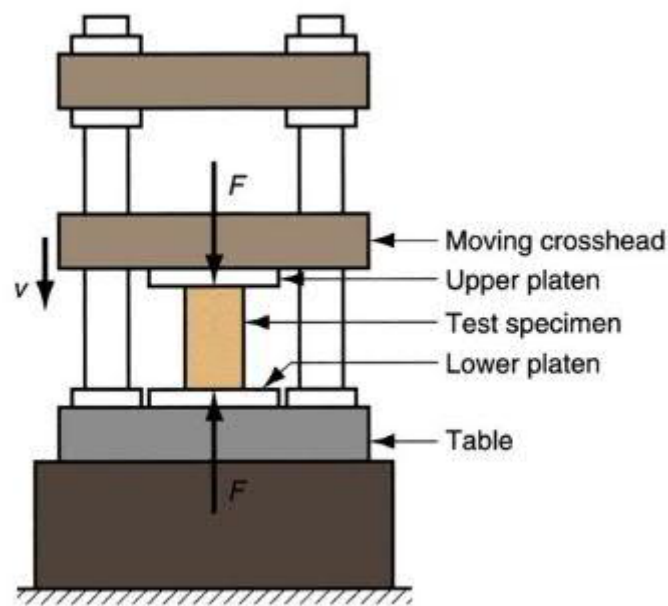


Figure 31. The principle of compression test. /55/.

$$\sigma_c = \frac{F}{A}, \quad \text{where } \sigma_c = \text{Compression stress}, \quad (7)$$

$F = \text{Force applied},$

$A = \text{Area of the cross – section}$

$$\varepsilon_c = \frac{\Delta L}{L_0}, \quad \text{where } \varepsilon_c = \text{Compression Strain}, \quad (8)$$

$\Delta L = \text{Change of length},$

$L_0 = \text{Initial length}$

$$E_c = \frac{\sigma_c}{\varepsilon_c}, \quad \text{where } E_c = \text{Young's modulus in compression}, \quad (9)$$

$\sigma_c = \text{Compression stress},$

$\varepsilon_c = \text{Compression strain}$

5.1 Strength of the Printed Material

Seven tensile test bars were manufactured as solid with Metal X regarding the standard ASTM E8, Standard Test Methods for Tension Testing of Metallic Materials. Four were manufactured in Markforged Boston premises, one in August 2018, and three in October 2018 rest three were manufactured in Wärtsilä's premises with Wärtsilä's Metal X. Markforged manufactured test samples were tested in the tensile test machine at VAMK, University of Applied Sciences, and Wärtsilä's manufactured samples were tested in Dekra. The test results were close to the Markforged material datasheet, 1050 MPa as sintered (Figure 32).

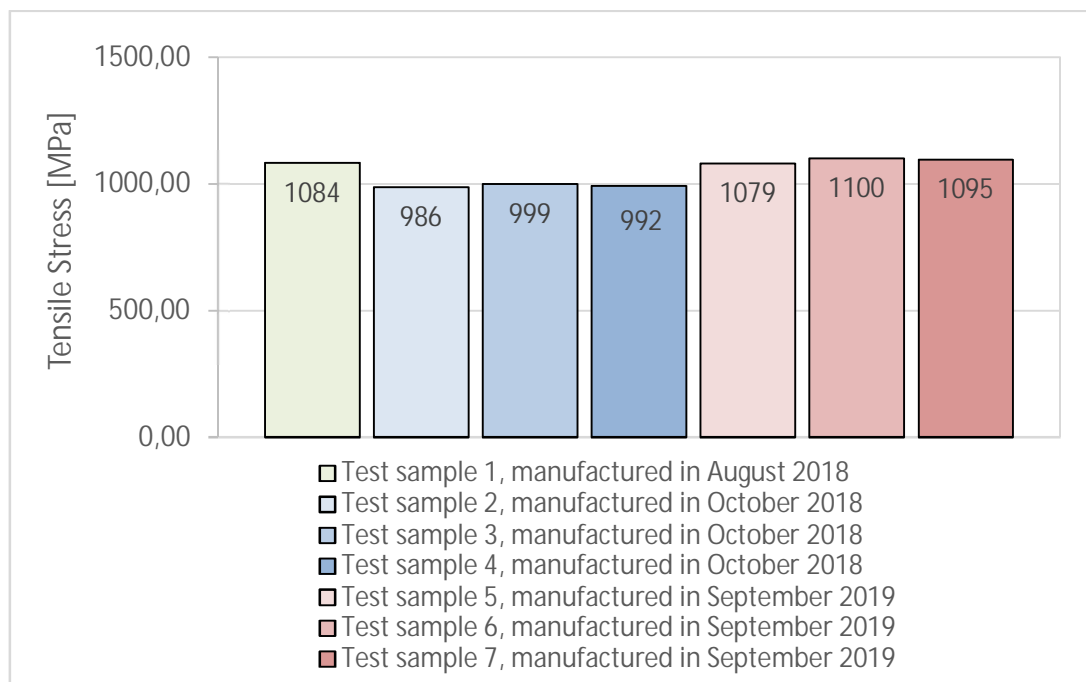


Figure 32. Maximum stress from solid test samples material strength tests.

Material investigation was done to test bars number one, three and six. The investigation shows that the porosity level is significant (Figure 33), the largest cavities in sample number one were almost $100\mu\text{m}$ and the largest cavity in sample number three was $187\mu\text{m}$ (Figure 34). In the same material investigation, hardness test of the samples was measured. The results were 350 to 355 in sample number one and 341 to 344 in sample number three in Vickers hardness VH10. It corresponds to the scale of 36 to 37 in Rockwell's HRC, a little harder than in the Markforged datasheet, 30 HRC as sintered.

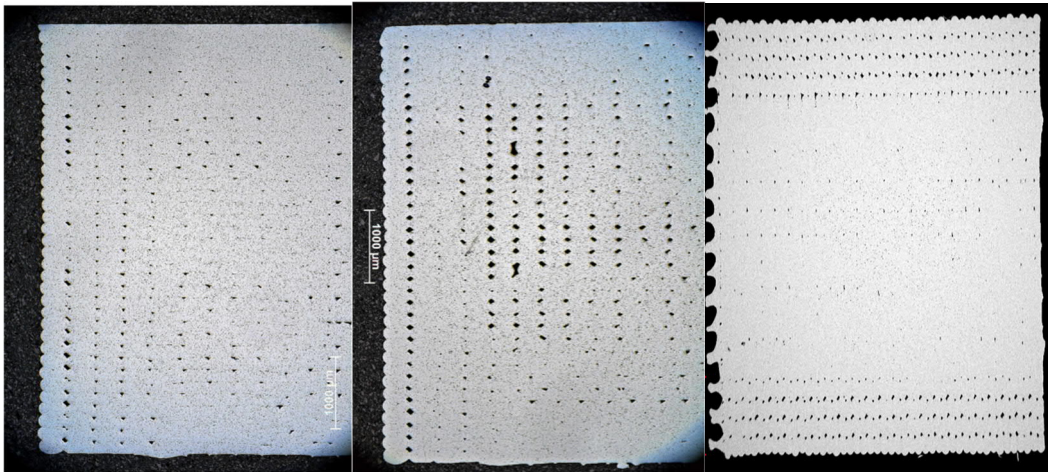


Figure 33. 1000 μm overview from the cross sections. Sample number one on the left printed August 2018, sample number three on the middle, printed October 2018 and number six on the right, printed September 2019.

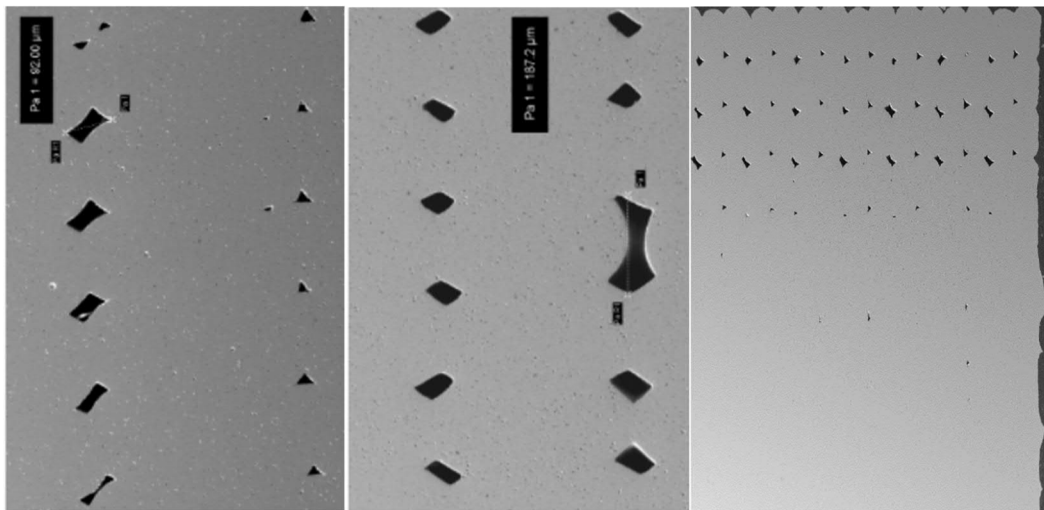


Figure 34. 100 μm close-up from the cross section. Sample number one on the left, sample number three on the middle and sample number six on the right.

Images above indicate that the changes in printing parameters have alter. These changes may have effect on the strength of the parts, by decreasing the porosity level of the part. However, in tensile strength the effect of these changes is minor.

5.2 Strength of the Printed Basic Geometry

The strength of the material 17-4 PH SS is good (Figure 32), however the material data from these tests cannot be used when simulating the strength of printed tools. The infill structure inside the printed part makes the part light but not as strong as when it is solid (Figure 35). Because of the infill structure, the weight loss compared to solid is rapid (Figure 36). With the sintering volume of Sinter-1, which is 1 200 cubic centimetres, the weight is 35 percent of solid volume.

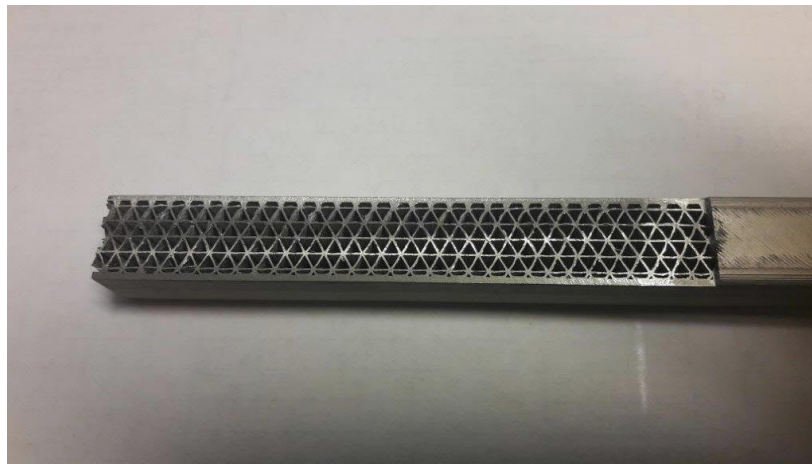


Figure 35. Printed & machined sample to demonstrate the sintered infill.

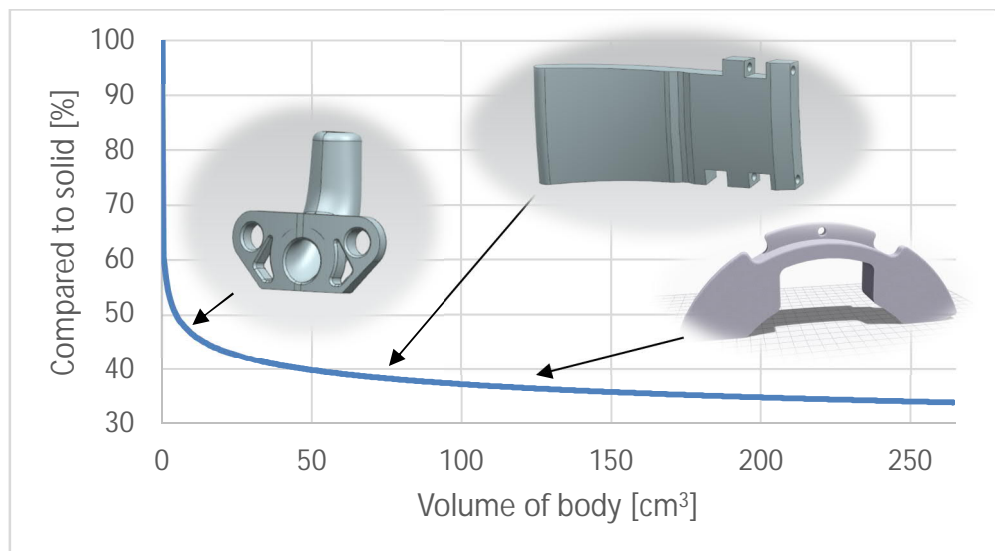


Figure 36. Weight reduction compared to solid part, which is a result of the infill structure inside the part.

For benchmark strength tests a tensile strength test, a 3-point bending strength test and a compression strength test were chosen. An additional test to simulate the actual user situation was carried out as a variation from the bending strength test. Because the samples manufactured with Metal X are not close to any other manufacturing result, due to the infill structure, the same kind of structure cannot be achieved with any other method. There are no standards to follow directly, and these tests are done with a trial and error method, standards are more like guidelines than direct rules in this research.

5.2.1 Tensile Strength

Tensile strength tests followed standard ASTM E8 and ISO 6892 by test speed and test conditions. The dimension of test samples was not from the standards because the standard is for homogeneous materials, which parts made with Metal X are not. The dimensions of the test samples were from 10 mm to 60 mm in height and 10 to 40 in width. Making test samples varies from each other, it can be seen how much the infills affects the strength of the part. Calculations of the strength of the test bars were done based on an internal view from Eiger, where printed part can be inspected layer by layer (Figure 37).

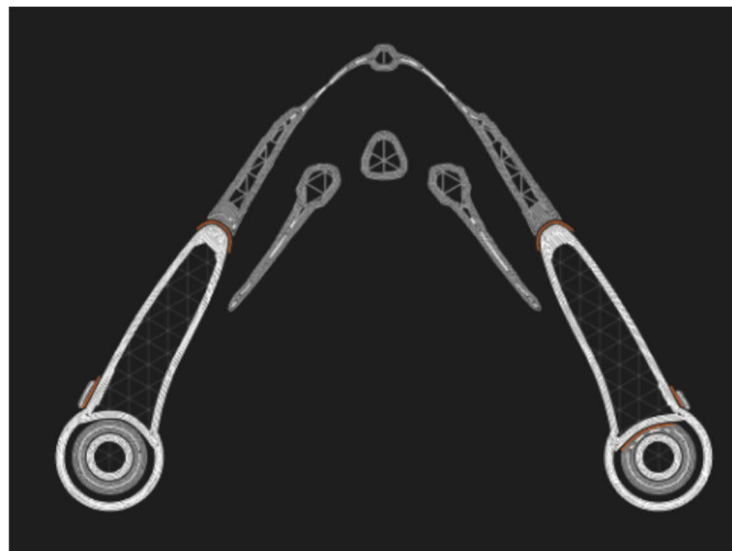


Figure 37. Internal view from Eiger, same part as in Figure 20 and in Figure 22 but from the layer 29. The white is the actual part material, the orange is a release material and the grey is a support material.

From Eiger the layers of solid material around the edges can be inspected precisely and how many triangles the infill consists of. Based on that, two different strength curves were made (Figure 38). The green curve shows the calculated strength when all printed metal in the cross-section was calculated so it also includes the infill structures. The red curve demonstrates when only the solid material on the outer walls of the sample is included in calculations.

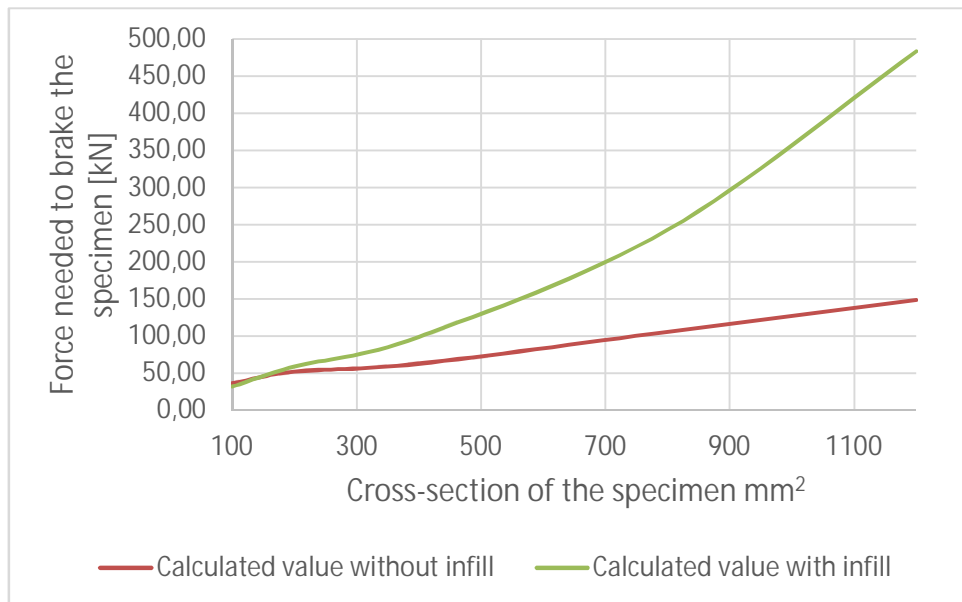


Figure 38. Calculated values based on the Eiger internal view. Two different calculations were made, infill included and not included in calculations.

Three test samples from every dimension were manufactured except the series TS1 which had four samples. The first series to manufacture was TS1 with a width and a height of 20 mm. TS1-1, TS1-2, and TS1-3 were printed in the same direction, but TS1-X in different (Figure 39). All the other dimensions were printed in the same direction as TS1-1, -2, and -3. A tensile strength test was done with two machines, Zwick/Roell Z100 and MTS810. Zwick/Roell Z100 had a maximum force

of 100kN and in MTS810 240 kN. The elongation data from samples were only possible to have with the machine Zwick/Roell Z100.

Table 1. Tested samples and their dimensions in tensile strength test.

Sample	Sample width [mm]	Sample thickness [mm]
TS1	20	20
TS2	40	20
TS4	20	40
TS7	20	60
TS10	10	10
TS11	20	10
TS12	10	20

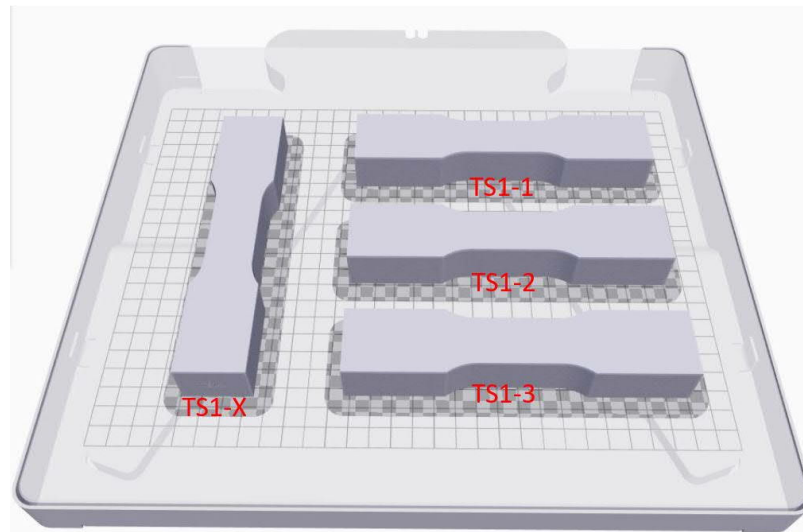


Figure 39. 20mm x 20mm test sample locations in print bed.

With the test samples with 20 mm width, the tensile strength test corresponded quite close to the calculated values without the infill attached. However, the sample TS1-X was closer to the calculated values with the infill attached (Figure 40).

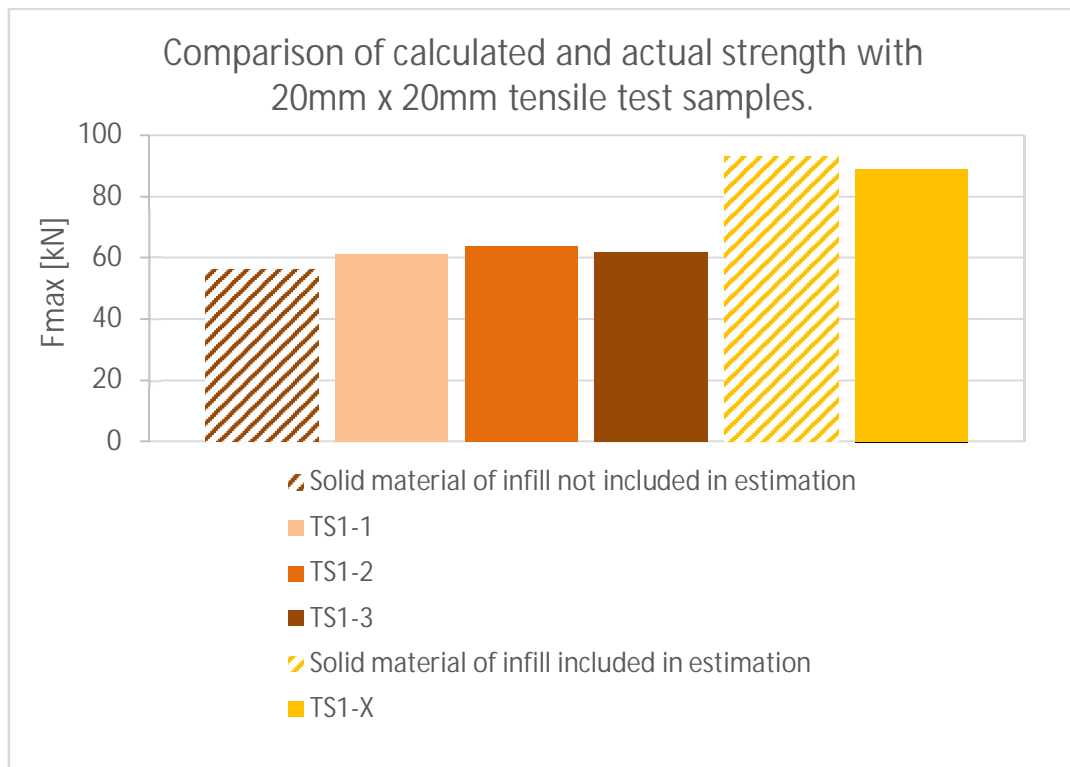


Figure 40. Comparison between calculation model and strength test values with samples TS1.

The specific elongation data from all the samples was not available due to the size of the samples and because some of the samples were broken outside the measurement zone (Figure 41. Test sample series TS11, where can be seen that one sample is broken outside the measurement zone, although the strength to break the sample did not deviate from others.). From the samples TS1-1, TS1-2 and TS1-3, the elongation data was available due a strain gauge, which was attached to the samples (Figure 42).



Figure 41. Test sample series TS11, where can be seen that one sample is broken outside the measurement zone, although the strength to break the sample did not deviate from others.

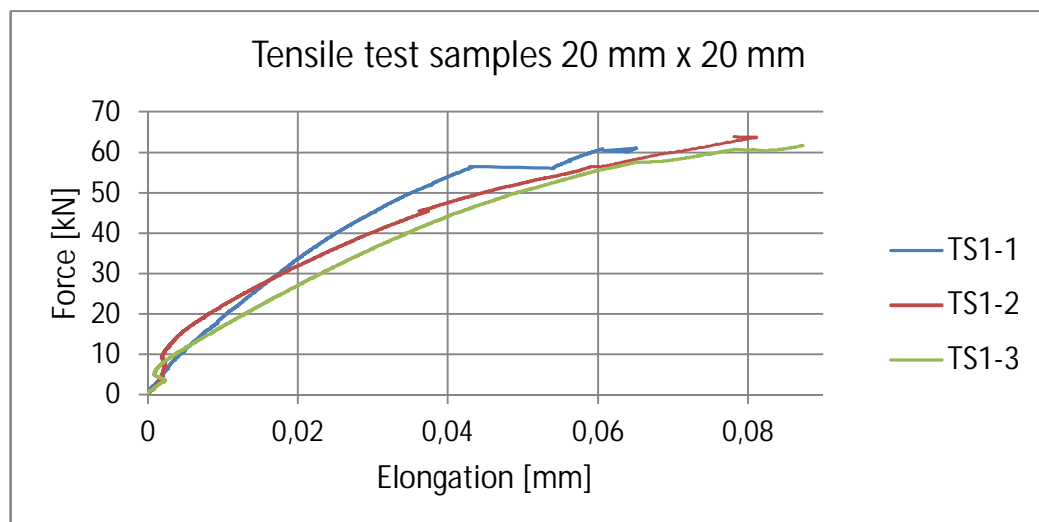


Figure 42. Elongation data from TS1-1, -2, and -3 test samples

The strength tests done correlate well for the calculated value when the infill is not included (Figure 43). It indicates that the infill inside the part has no or only minimum effect on the strength of the sample, except the sample TS1-X which correlated more to the calculations where the infill was attached. The bigger the cross-section of the sample is, the lower is the stress value of the sample (Figure 44).

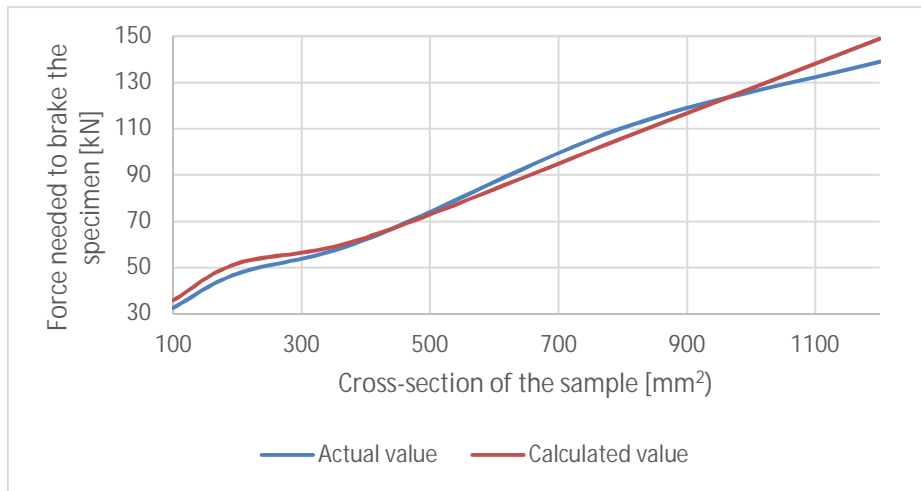


Figure 43. The actual and calculated break force for the tensile test samples.

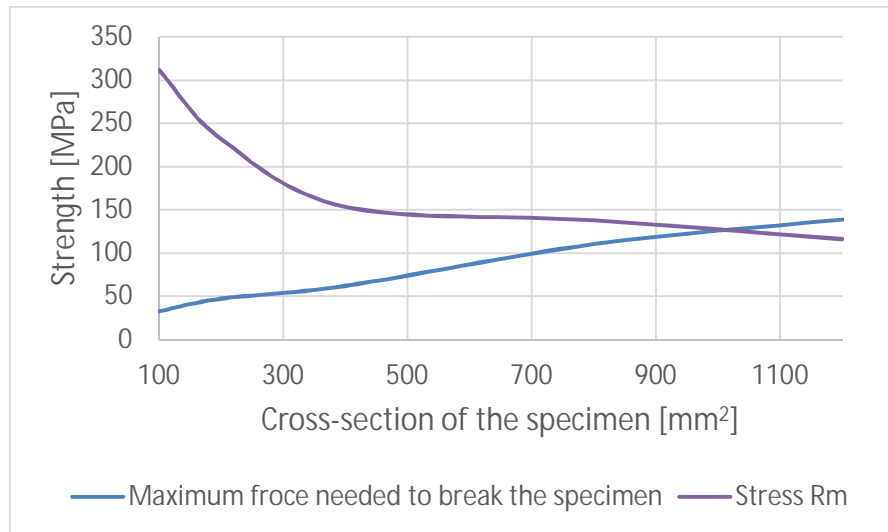


Figure 44. Relationship of maximum force and stress with 3-point bending samples.

5.2.2 3-Point Bending Strength

In the 3-point bending strength test, the standard to follow was ISO 7438, which is a bend test standard for Metallic material. The standard gave directions for the dimensions of the test samples and the dimension for the space between the supports, the procedure, and the formulas. The samples were designed in three different sizes.

Table 2. Test samples and their dimensions in 3-point bending strength test.

Sample	Sample width [mm]	Sample thickness [mm]
3BS7 & 8	7.25	7.25
3BS1 & 2	15	15
3BS3 & 4	22.75	22.75

Six samples in every dimension, except eight samples in size 15 mm x 15 mm. All except two in the size 15 mm x 15 mm (Figure 45) were printed in the same X-direction and the two in Y-direction, 50 percent of them were bent in a Z-direction and the rest in a Y-direction. The samples in categories 3BS1, 3BS3, and 3BS7 were bent on Z-direction (Figure 46) and the samples 3BS2, 3BS4, and 3BS8 on Y-direction (Figure 47). The printing direction to all bending test samples was in XY-plane.

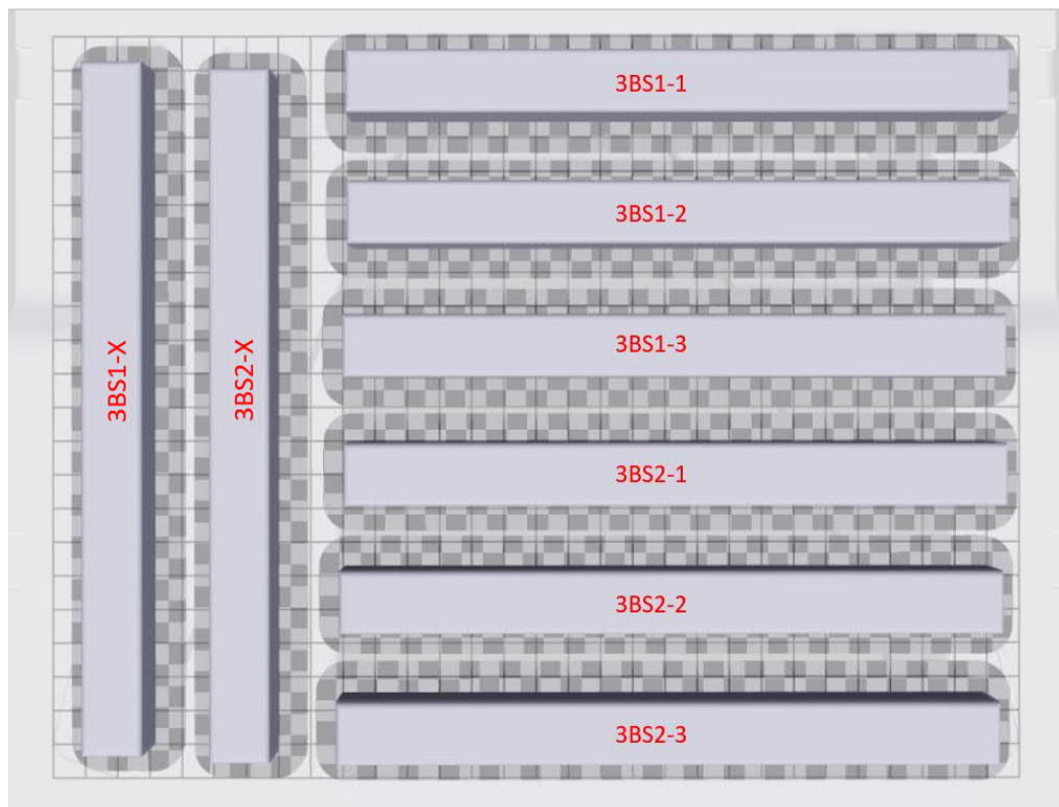


Figure 45. Printing directions for size 15 mm x 15 mm.



Figure 46. Bending direction Z for sample series 3BS1, 3BS3 and 3BS7.

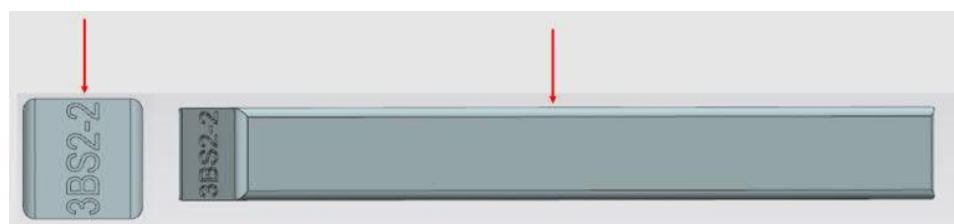


Figure 47. Bending direction Y for sample series 3BS2, 3BS4 and 3BS8.

The test machine used to test the bending test samples was Wolpert Testa U-30. The machine cannot measure the elongation, the only precise information from the test, was the maximum force applied. The support space dimension was from the standard ISO 7438, which for example with the samples in series 3BS8 and 3BS7, was 78.25 mm. The samples were placed between the supports (Figure 48) and the load was applied to the middle of the samples until the sample was broken (Figure 49).



Figure 48. Test sample 3BS8-3 before loading.



Figure 49. Test sample 3BS8-3 after loading.

With all the samples, where the bend direction was Y-direction (Figure 47) the force needed to break the sample was bigger (Figure 50) except in the sample BS1-X where the value was more closely to the samples bended in Y-direction even though it was bended in Z-direction (Figure 51).

In the calculations the maximum load applied as in F_{max} was from the machine's log, and from the photos, before and after the load, can be calculated the bending angle of the break and therefore estimate the elongation of the sample (Figure 48 & Figure 49). The break angle of the test samples was from 4 degrees to 13 degrees, depending on the sample dimensions and the bending direction. Flexural stress (Figure 52) and Flexural modulus as the Young's modulus (Figure 53) also vary depending on the sample dimensions and the bending direction. Formula 4 was used to calculate the flexural stress of the samples and formulas 5 and 6 to calculate the Young's modulus.

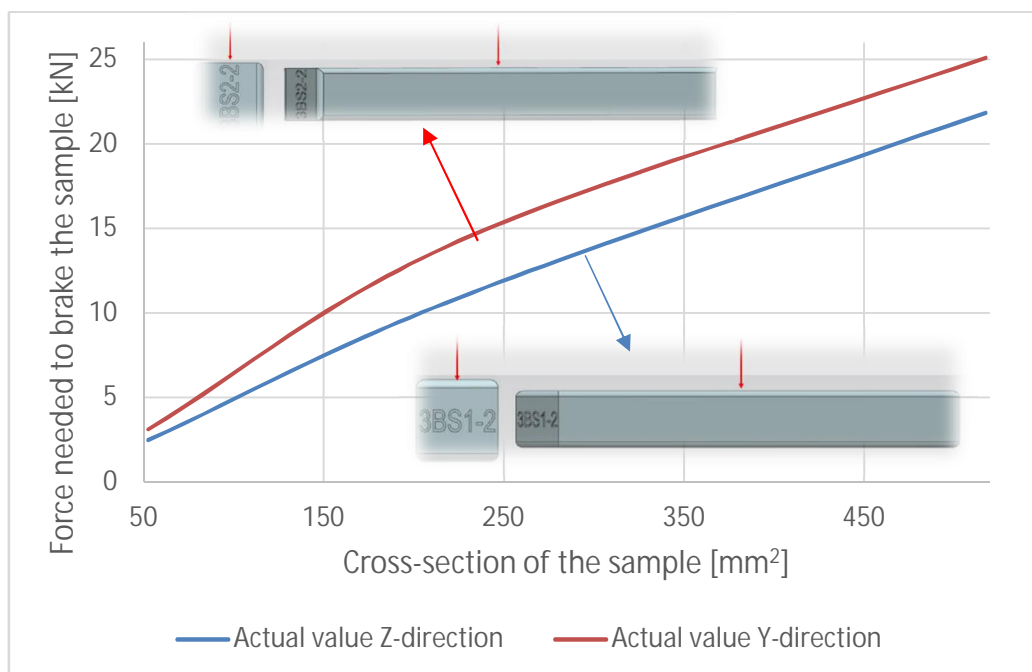


Figure 50. Three-point bending test results.

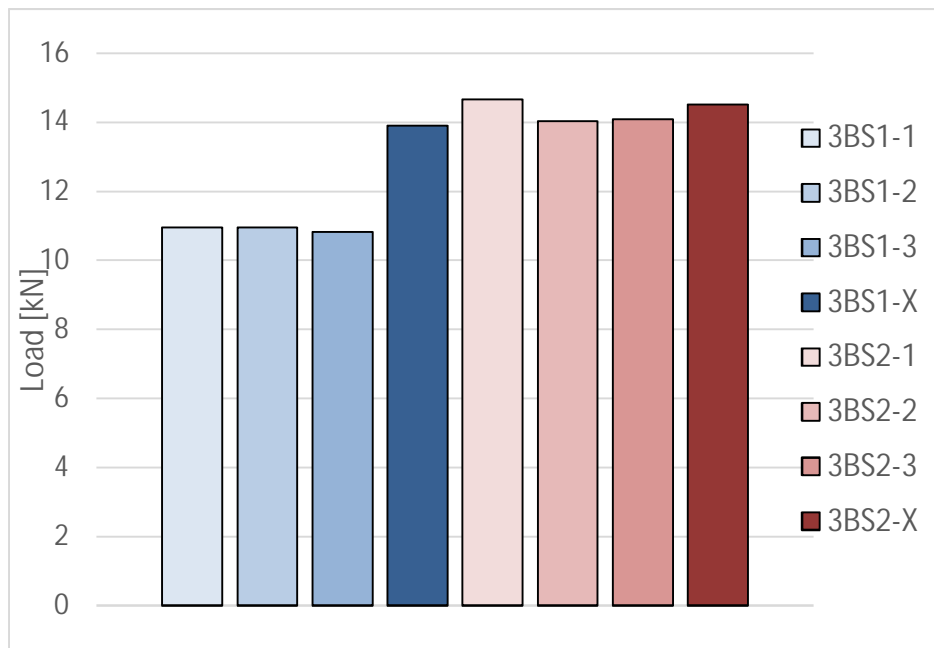


Figure 51. The breaking load in the 3-point bending test, with 15 mm x 15 mm samples.

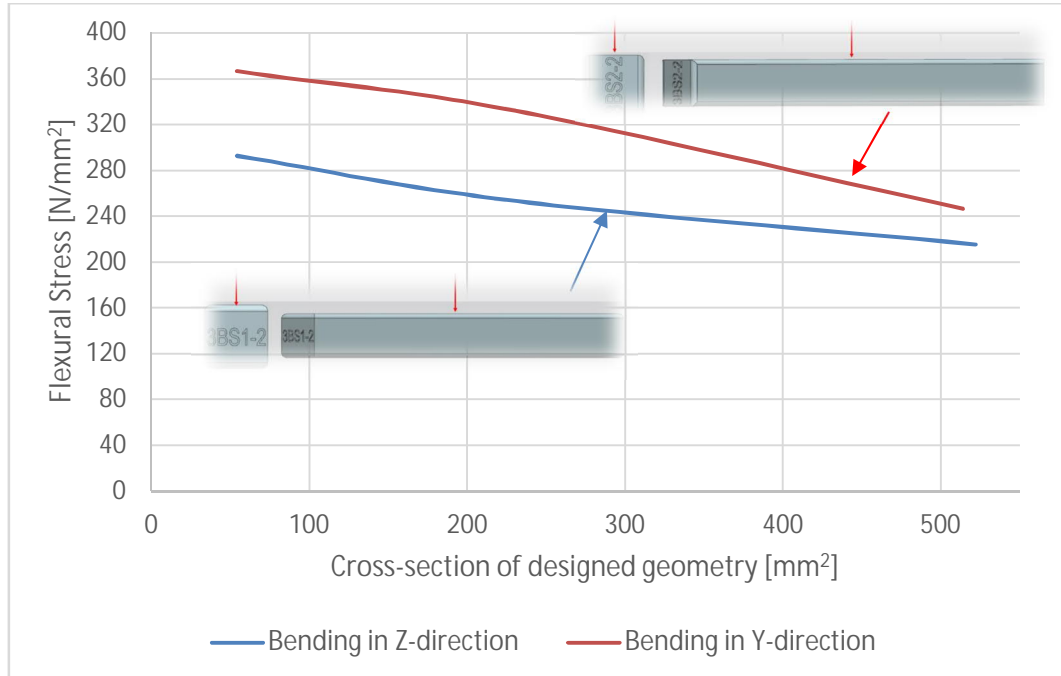


Figure 52. Flexural stress compared to cross-section of 3-point bend samples.

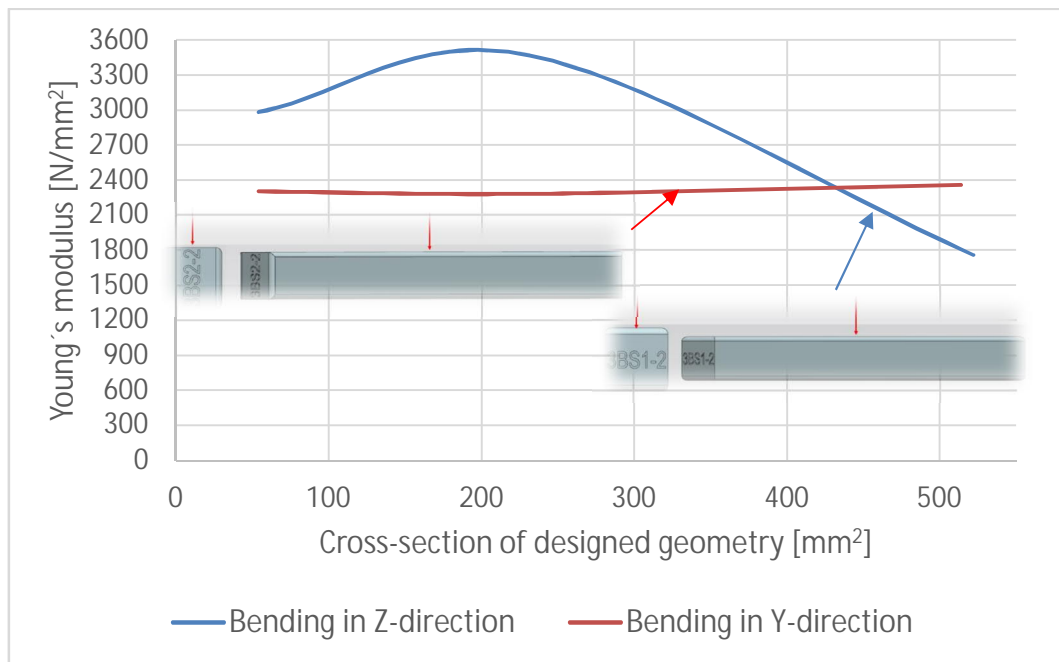


Figure 53. The Young's modulus compared to cross-section of 3-point bend samples.

5.2.3 Compression Strength

Compression samples were made only in two different sizes, three sample in both sizes (Figure 54).

Table 3. Test samples and their dimensions in compression strength test.

Sample	Sample dimension [mm]	Sample length [mm]
CS1	20	20
CS2	30	60

The first series CS1 had a length/diameter ratio of one and the second series CS2 had a length/diameter ratio of two. The maximum strength of series CS2 was twice as much as in series CS1 (Figure 55). These tests indicate that the change in length/diameter ratio from one to two affects the maximum load by doubling the load.



Figure 54. Compression test samples after the test, CS1 on the left and CS2 on the right.

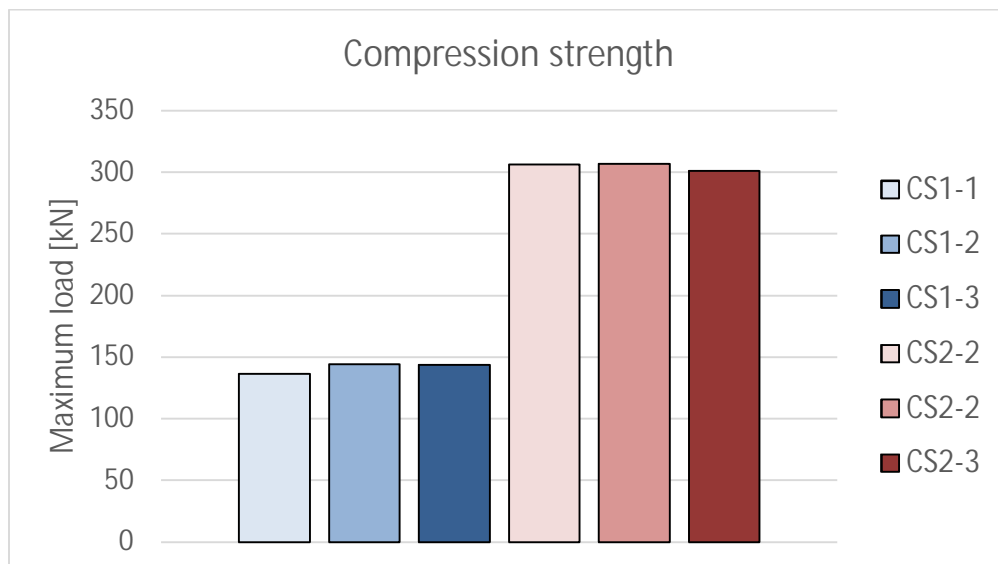


Figure 55. Maximum loads of compression test samples.

From that maximum load data, using compression stress formula (7) the compression stress of the samples can be calculated (Figure 56). The compression test in both samples are more or less the same, with CS1 $456,77 \pm 11,5$ MPa and with CS2 $432,70 \pm 4$ MPa. The compression test was done to inspect the effect of the length/diameter ratio.



Figure 56. Compression stress chart for compression test samples in series CS1 and CS2.

6 DESIGN FOR ADDITIVE MANUFACTURING FOR ADAM IN STRENGTH PERSPECTIVE

There are certain design limitations and strengths in every additive manufacturing technique and every material. This chapter the focus is on designing for Metal X Basic design rules that apply to FDM printers, apply to Metal X. Markforged offers a design guide for Metal X, where part dimensions, overhangs, hole and post diameters, and basic design rules can be found. The guide also includes basic optimizing rules for washing and sintering parts, and post-processing of printed metal parts. /56/.

6.1.1 Part Dimensions

The maximum printable end part size is 250 mm in X-direction, 183 mm in Y-direction and 150 mm in Z-direction/57/. However, if using Sinter-1 the above-mentioned maximum part size is not correct, the maximum part size of Sinter -1 is 235 mm in X-direction and 68,3 mm in Y-direction. With Z-direction there are two restraining sizes, the overall maximum size in Z-direction is 80 mm if the part fits the radius of 55,5 mm centered, otherwise the maximum part size in Z-direction is 65,5 mm, larger parts need to be sintered externally or in Markforged Sinter-2, which is much larger than Sinter-1 (Figure 57).

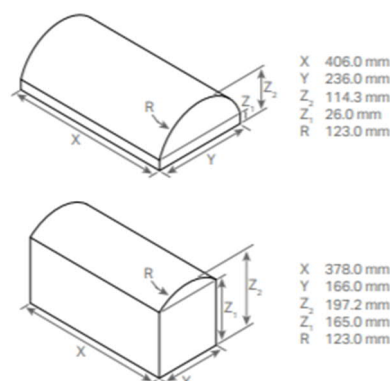


Figure 57. The maximum dimensions with Sinter 2 /57/.

The minimum designable part dimensions are 2.8 mm in X- and Y-direction and 1.7 mm in Z-direction, dimensions smaller than these may fail because the size of the filament and thin walls may cause weakness to the structure /56/.

For the layer height, there are two options to choose: 50 microns or 125 microns. The 50-micron layer height is still in the Alpha test phase, so the print may not be successful if printed with 50 microns. A smaller layer height means a better surface quality, and the printer can produce much more accurate details, but on the other hand, printing will take more time. A ratio for printing time and layer height is linear. The printing time will be doubled if the layer height is doubled /58/.

6.1.2 Surface Quality

Surface quality was measured in three different angles with three different post processing done after printing. The same sample was printed in angles 0, 45 and 90 degrees (Figure 58). The samples were divided into four sections and every section had a different surface treatment. The first surface was sanded before wash, the second one was sanded before sintering and the third is as sintered surface, the fourth section was designed to be machined but machining was left out. The sanding was done with basic sanding paper with grit of 600, both sections, which were sanded, had an equal amount of sanding, four equal traction.

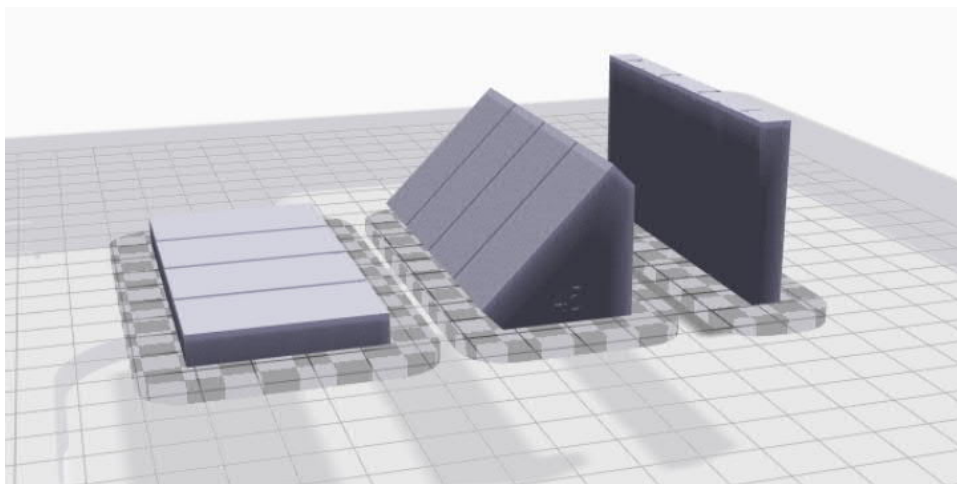


Figure 58. Surface roughness test pieces. 0 degree on the left, 45 degree on the middle and 90 degree on right.

The outcome from this test was that sanding before the wash reduced both values, Ra and Rz in 0 and in 90 degrees, however with 45 degrees it had a negative effect on the Ra value and no effect at all on the Rz value. Sanding before the sintering on the other hand had no effect or negative effect on the Ra value but on the Rz value it had a degrading influence except with 45 degree sample it had no effect (Figure 59). From these figures, it can also be seen that the Ra and Rz values as sintered increase significantly from 0 degree to 45 and 90 degrees.

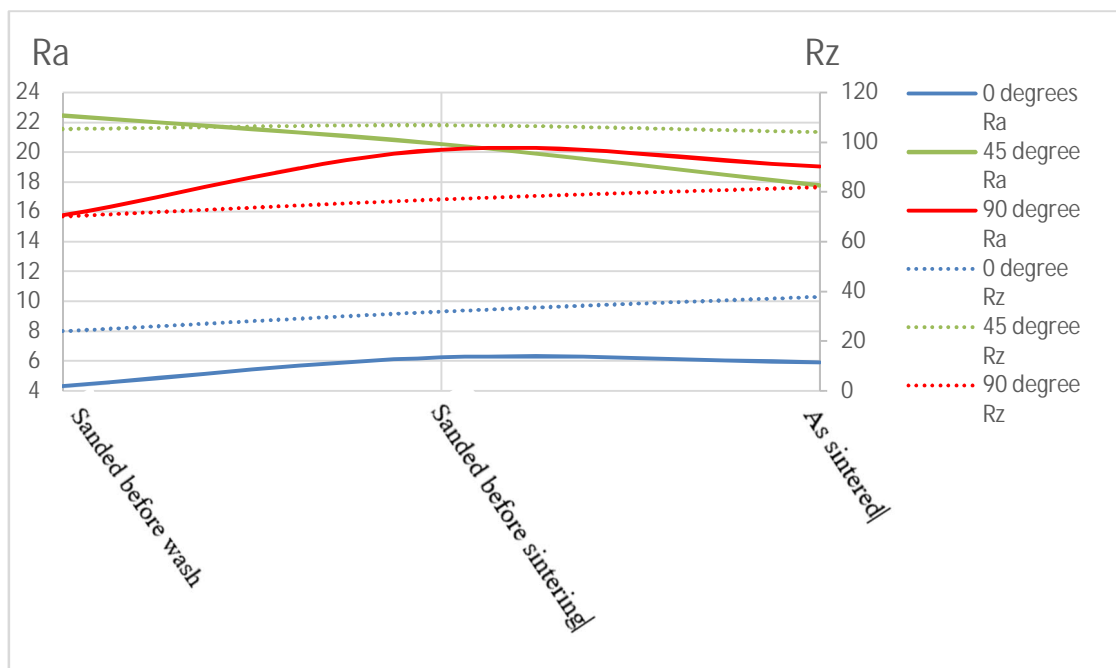


Figure 59. Measured Ra and Rz values. On the left Ra values and on the right Rz values.

This was a small test, which indicates that there is a chance to reduce the surface roughness in certain directions. If more accurate values are needed, the test method must be rethought, and more samples must be manufactured and tested.

7 SUMMARY

The tests indicate that plenty of research must be done before there is a trust for material properties of Metal X printed parts. Even though the sampling was small, it indicated the variation in the strength of the samples, which must be considered when calculating or optimizing the structure. However, in some cases where the strength is not so critical or it is not needed, parts manufactured with Metal X can be utilized without doubts.

The bigger the samples are, the more significant is the impact of the infill, because the solid material at the outer edges is constant, however there is an option to choose the layers of solid material in outer edges but that is something to investigate later. The tests indicate that the infill in certain printing directions has no impact, but in some, it has a huge impact. When inspecting the tensile test pieces, the force needed to break the sample TS1-X was 88,92 kN and in TS1-1 it was 61,063 kN. The only difference between these test bars was the printing direction because of that change in printing direction (Figure 39), the infill geometry was entirely different between those bars (Figure 60).



Figure 60. Cross-section views from Eiger, TS1-X on the top and TS1-1 on the bottom. This demonstrates that the infill structure has a huge impact to the strength.

Calculated estimations, which were based entirely on the solid material in the cross-section of the test bar, indicates that when the extruded material is according to the

rod as in TS1-1, it has close to zero impact on the tensile strength. The calculated estimation where only the solid material in the outer surface was considered and not the infill was approximately 63,01 kN, and the average break force in samples TS1-1, TS1-2 and TS1-3 was 62,207 kN. When the extruded material in the infill is against the rod, as in sample TS1-X, the brake force was closer to the calculated estimation where the solid material in the infill was considered, 88,92 kN in TS1-X and 99,18 kN in the calculated estimation. From the close-up view, the difference between the infill of the test bars can be seen (Figure 61), the only difference was the direction of the infill. The same kind of results can be seen from other dimensions, in the sample series TS4 the average strength was 110,41 kN when calculated strength without infill attached was 105,94 kN and in sample series TS7 the average strength was 139,01 when the calculated strength was 148,89 kN.

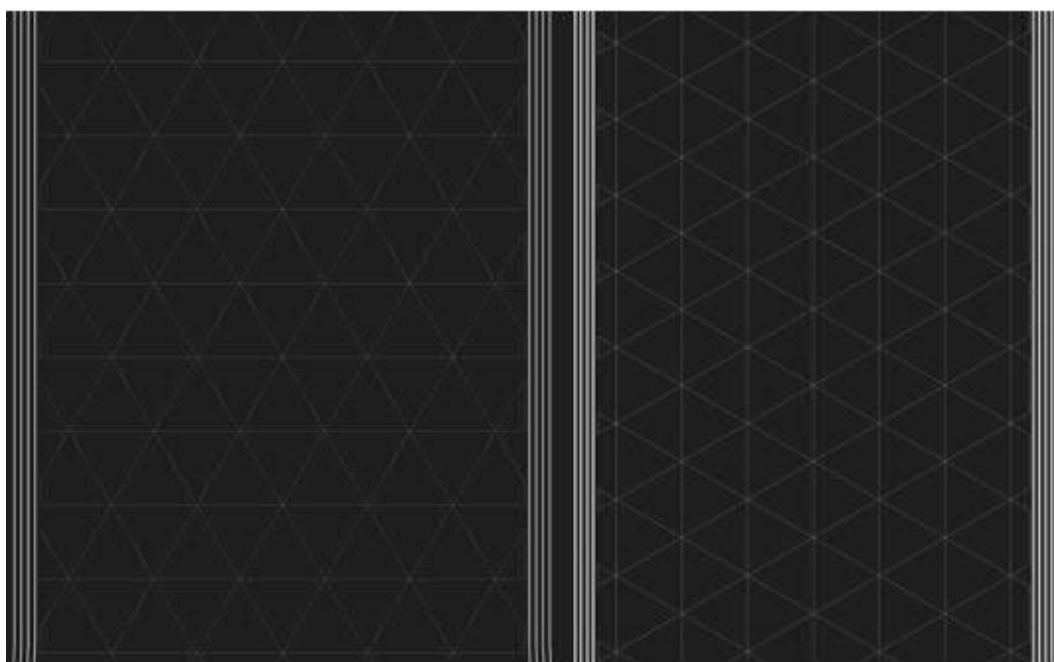


Figure 61. Close up of cross-section views from Eiger, TS1-X on the left and TS1-1 on the right.

The test series TS2, which was the only series where the thickness of the test samples was increased to 40 mm, the results were quite different. Two of the samples were quite well in line with the calculations, approximately 90,5 kN when calculated value was 84,4 kN but the sample TS2-2, which had the strength value of only 36,1 kN, there was no noticeable difference between the series TS2 samples.

The results from bending strength tests indicate that the effect of bending direction compared on printing direction is remarkable. Strength when the bending force direction is different than printing direction (Figure 47) was greater, however there were fluctuation between the dimensions.

Table 4. The difference in bending direction.

Sample dimension	Average maximum force in bending direction Z [kN]	Average maximum force in bending direction Y [kN]	Percentage difference
7,25 x 7,25 mm	2,5	3,1	25,6
15 x 15 mm	10,9	14,3	30,7
22,75 x 22,75 mm	32,8	37,7	14,9

However, with the samples 3BS1-X and 3BS2-X, which were printed in different orientation, the difference was only 4 percent. Only difference with these samples was the infill structure (Figure 62 & Figure 63).

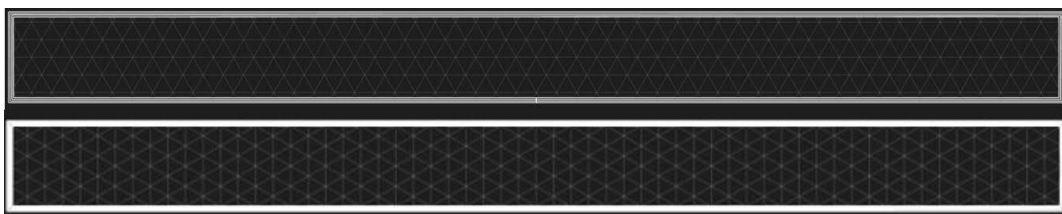


Figure 62. Cross-section views from Eiger, 3BS1-1 on the top and 3BS1-X on the bottom.

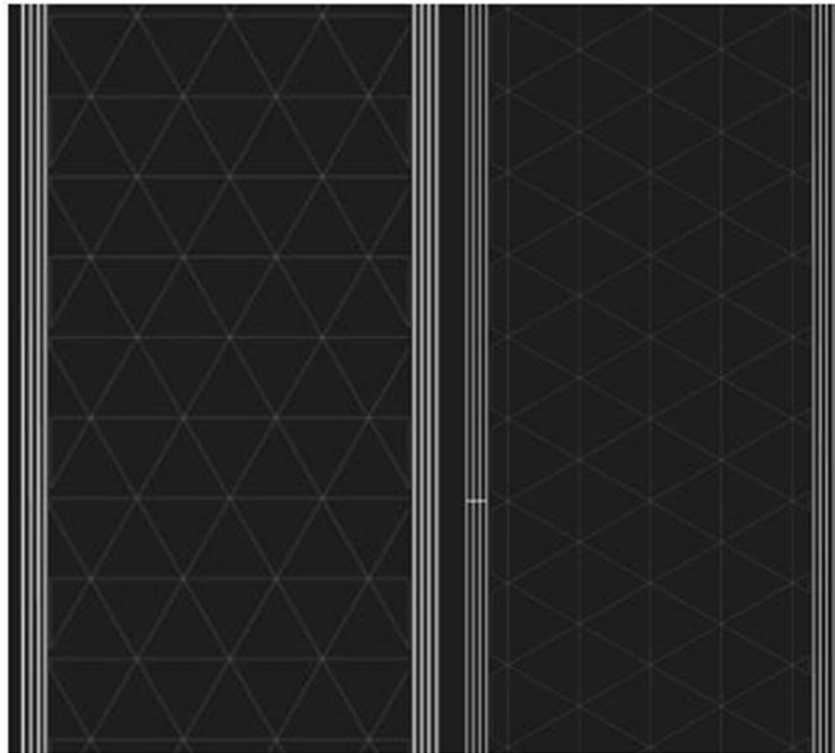


Figure 63. Close up from cross-section views from Eiger, 3BS1-1 on the right and 3BS1-X on the left.

Even though the bending angle was used to calculate the flexural stress and Young's modulus, which is not the accurate measurement method, it gives a good benchmark that samples where the bend force is different than the print direction are more durable and stable.

The tensile test results indicate that if the height of the sample is increased it will have more strength; however, this is due to the solid wall thickness of 1 mm on walls and 0.6 mm on roof and floor. The bending test on the other hand indicates that the bend direction has more strength if the bend direction is different from the print direction. Both tests also indicate that the printing direction in X and Y plane has a huge impact on the strength.

8 CONCLUSIONS

Parts manufactured with Metal X do not have the same strength as can be achieved with other methods, for example with PBF or turning and milling from billet material. However, this lack of strength is only due to the infill structure, with the printed material itself the same strength can be achieved if printed as solid. Because of this infill structure, Metal X manufactured parts cannot be used in critical applications. However, there are certain applications where the strength of the part is not the priority for example measuring tools, jigs and fixtures (Figure 64, Figure 65 & Figure 66). These parts may have certain shapes, which cannot, or it would be too expensive to manufacture traditionally but high strength requirements are missing. Certain applications where the material requirement is metal or plastic and composite prints would not last.

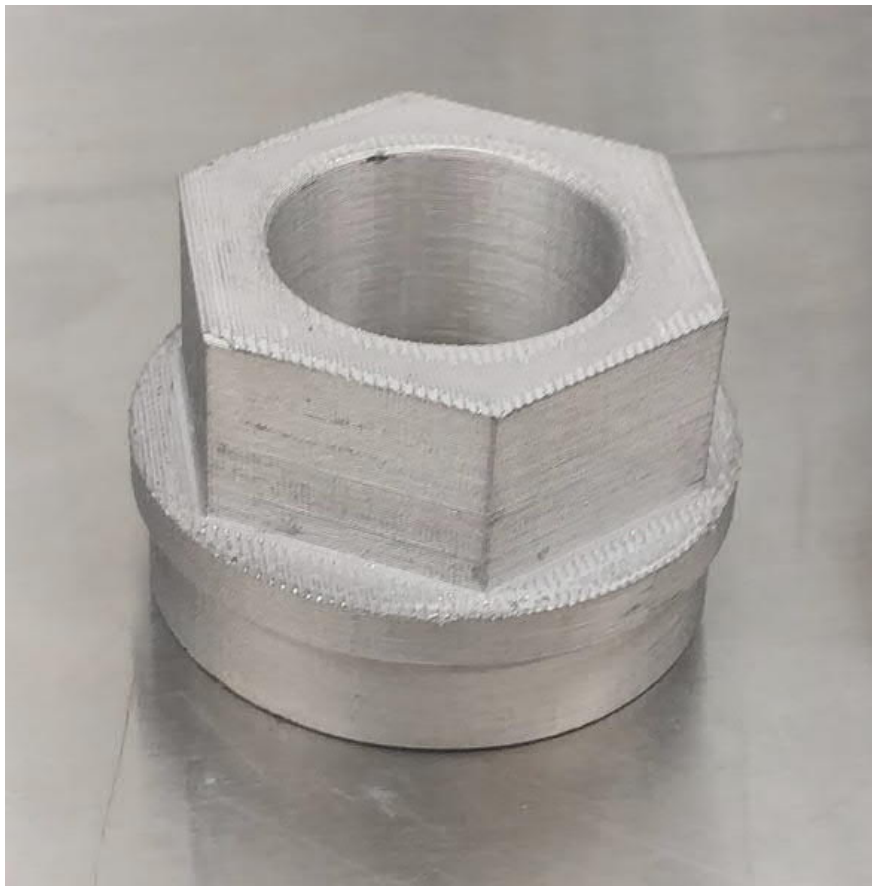


Figure 64. Tightening tool applications manufactured with Metal X.

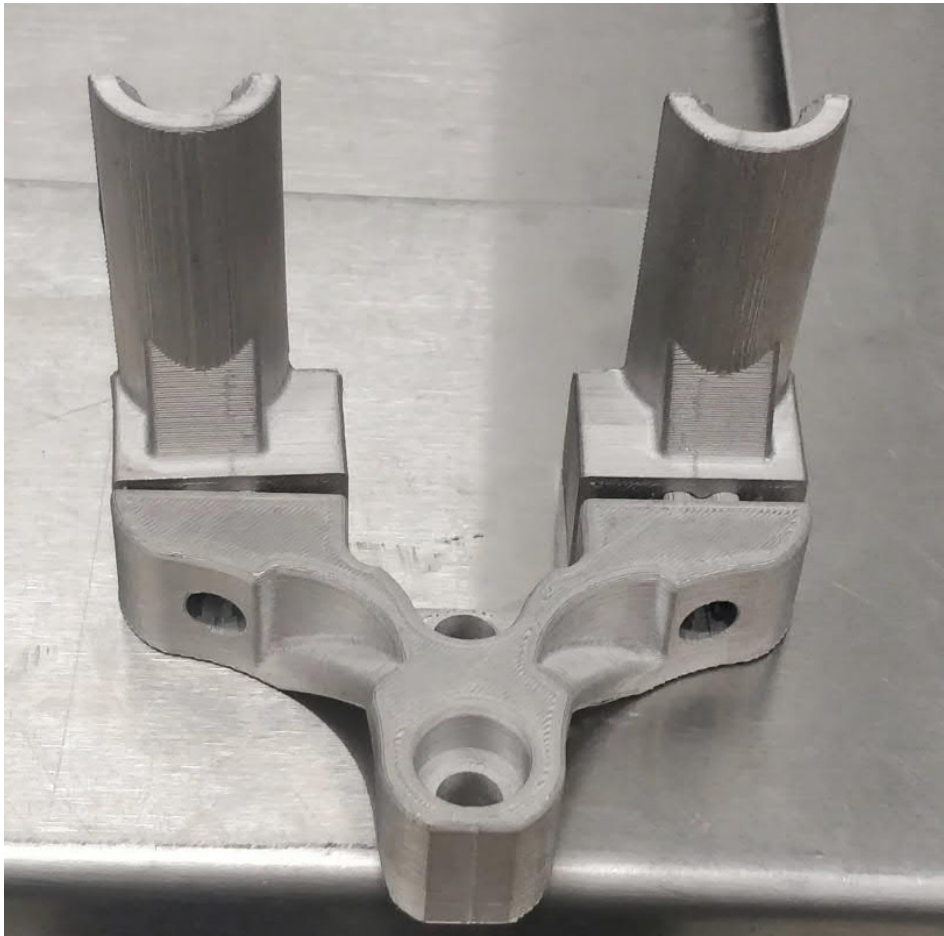


Figure 65. Gripper application manufactured with Metal X.

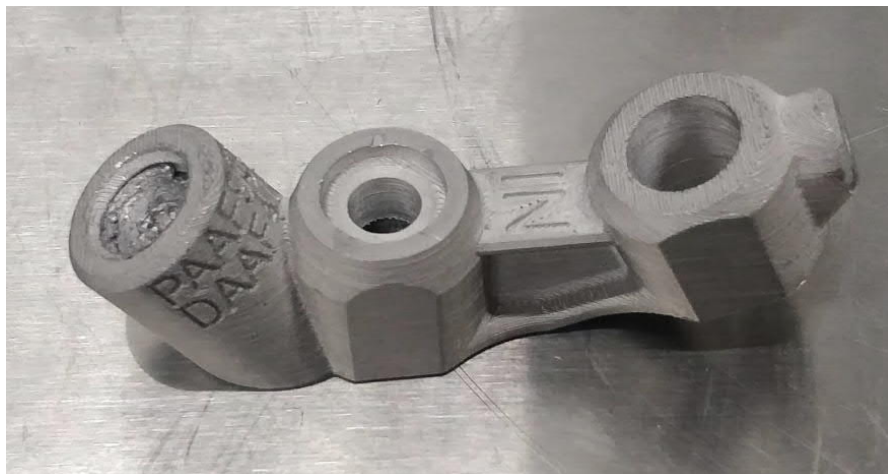


Figure 66. Measuring tool application manufactured with Metal X.

Much more tests need to be done, to assure that there are no samples like TS2-2, which had only third of the strength that other samples in that category had. If there is even the slightest doubt that the part may not have the strength designed, it may not be used for example in the factory for parts which have strength requirements. Samples need to be built in different angles on the print table, to achieve the best angle for strength. Parts need to be printed with different heights and widths to gain more data from the effects of dimension change, and to find the optimal strength/print time diameter for different applications.

Different kind of tests need to be done, for example cyclic loading-unloading test, to gain the knowledge from plastic deformations. In a cyclic loading-unloading test, the part is exposed to certain stress and released several times. The elongation data from that test is collected and the changes in the elongation reveal the possible plastic deformation in the part. Tests with modified part structure can be done, for example a part where a thin strip from the body is cut away (Figure 67). In traditional manufacturing and for example in L-PBF, that modification would weaken the part, but when manufactured with Metal X, the part is most likely to be strengthened. The reason for increased strength is in the structure of the part, in the increased amount of solid material located in outer walls (Figure 68).



Figure 67. Extruded strip from a body, which most likely increase the strength of the part.

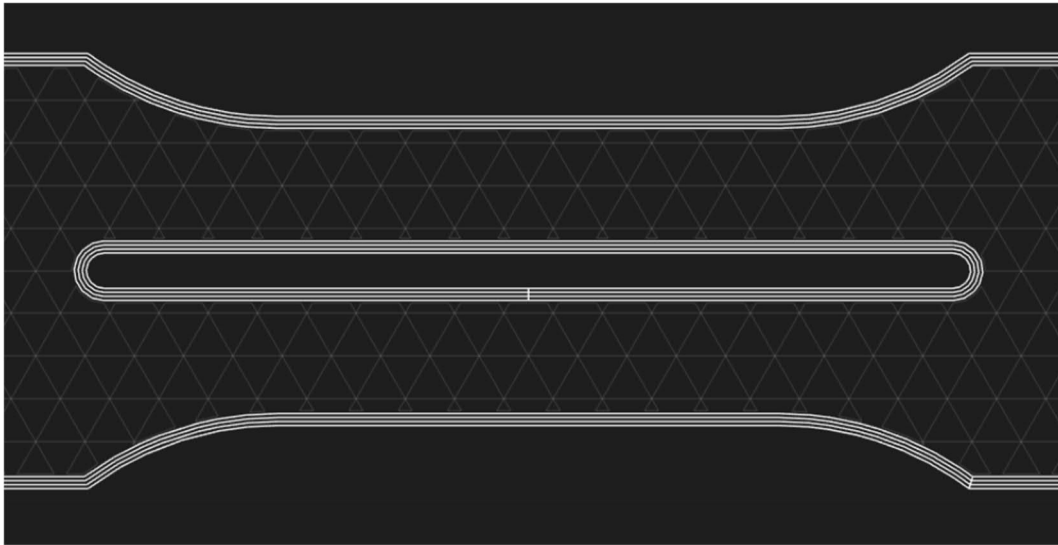


Figure 68. Cross section from the part where the strip is extruded. Increased amount of solid material in outer walls is very visible.

Based on the previous calculations, the part would most likely have a tensile strength of approximately 74 kN, when the strength without the strip extruded was approximately 62 kN. The increase in strength is a direct cause of the increase of solid material in outer walls. However, this might cause that the part is broken right next to where the solid material in the cut strip ends. One method to increase the strength of the part is by increasing the number of solid layers (Figure 69). However, it will directly increase the printing time and cost.

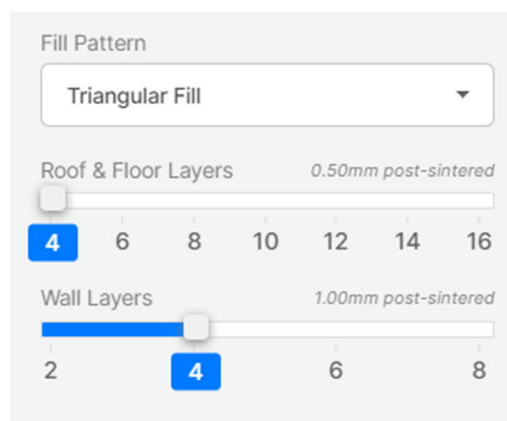


Figure 69. Infill settings from Eiger.

The Surface roughness tests and the effect of the surface roughness to the strength must be inspected; however, surface roughness may only have effect on the fatigue strength of the samples. However, in some applications the surface quality has a crucial impact on the functionality of the part. If printed parts are ever considered to be placed under a lot of cycling stresses, a fatigue strength test must be done.

The effect of the different printing directions must be examined to find the effects of different directions. The small sampling in this thesis was enough to indicate that the printing direction in X- and Y-plane affects the strength with this method. Different shapes must be examined and tested, for example, rounded edges, if there is any effect on the strength of the parts. Holes in the sample must be inspected. In traditional manufacturing, if holes are manufactured in the part, it will weaken the part but in Metal X manufactured parts the result might be the opposite. This plausible strengthening result might be due to the outer walls, if there is a hole in the part, it has more solid material around the sample.

This thesis demonstrated that the parts manufactured with Metal X are suitable for non-critical components where the strength requirements are not the main requirement. Differences in the samples and the printing directions were found, and the impact of the printing direction in the X- and the Y-plane was much higher than originally expected. The strength of the samples correlates fairly well when the solid material on the outer perimeter is only included in the strength calculations, in some directions. The 3-point bending tests indicate that the bigger the cross-section of the part is, the less the flexural strength is. The Young's modulus in a certain direction was steady, but in another direction, it was fluctuating.

REFERENCES

- /1/ About Wärtsilä. Wärtsilä Web Pages. Accessed 13.9.2019. <https://www.wartsila.com/about>
- /2/ History of Wärtsilä. Wärtsilä Web Pages. Accessed 13.9.2019. <https://www.wartsila.com/about/history>
- /3/ Wärtsilä's Smart Technology Hub. Wärtsilä Web Pages. Accessed 10.7.2019. <https://www.wartsila.com/sth>
- /4/ Strategy of Wärtsilä. Wärtsilä Web Pages. Accessed 9.7.2019. <https://www.wartsila.com/about/strategy>
- /5/ Wärtsilä solutions for Marine and Oil & Gas Markets. Brochure 2018. Accessed 10.7.2019. <https://www.wartsila.com/docs/default-source/marine-documents/segment/brochure-marine-solutions.pdf>
- /6/ Wärtsilä Energy Business. Wärtsilä Web Pages. Accessed 9.7.2019. https://wartsila.sharepoint.com/sites/compass/energy_business/Pages/default.aspx
- /7/ Wohlers associates INC. 2019. USA. Wohlers Report 2019 – 3D Printing and Additive Manufacturing State of the Industry – Annual Worldwide Progress Report
- /8/ ISO/ASTM 52900:2015. Additive manufacturing – General principles – Terminology. International Organization for Standardization. 2015
- /9/ About Additive Manufacturing, The 7 categories of Additive Manufacturing, Powder Bed Fusion. Loughborough University Additive Manufacturing Research Group Web Pages. Accessed 26.9.2019. <https://www.lboro.ac.uk/research/amrg/about/the7categoriesofadditivemanufacturing/powderbedfusion/>
- /10/ Additive technologies compared, Metal 3D Printing. 3D HUBS Web Pages. Accessed 26.9.2019. <https://www.3dhubs.com/guides/metal-3d-printing/>

/11/ Varotsis, A. Introduction to Metal 3D printing. 3D HUBS Web Pages. Accessed 25.12.2019. <https://www.3dhubs.com/knowledge-base/introduction-metal-3d-printing/#characteristics>

/12/ Stevenson, K. 2019. Velo3D's Incredible Metal 3D Printing Process. Fabbaloo 3D Printing News Web Pages. Accessed 26.12.2019. <https://www.fabbaloo.com/blog/2019/7/9/velo3ds-incredible-metal-3d-printing-process>

/13/ Varotsis, A. Introduction to Binder Jetting 3D printing. 3D HUBS Web Pages. Accessed 25.12.2019. <https://www.3dhubs.com/knowledge-base/introduction-binder-jetting-3d-printing/>

/14/ About Additive Manufacturing, The 7 categories of Additive Manufacturing, Directed Energy Deposition. Loughborough University Additive Manufacturing Research Group Web Pages. Accessed 26.12.2019. <https://www.lboro.ac.uk/research/amrg/about/the7categoriesofadditivemanufacturing/directedenergydeposition/>

/15/ Teollisuuden 3D-tulostus. 2019 Lappeenranta University of Technology. 2019. Me3DI Lectures.

/16/ Petch M. 2017. CES 2017 Markforged Metal X brings 3D Metal Printing to the desktop. 3D Printing Industry.

/17/ About Additive Manufacturing, The 7 categories of Additive Manufacturing, Material Extrusion. Loughborough University Additive Manufacturing Research Group Web Pages. Accessed 26.12.2019. <https://www.lboro.ac.uk/research/amrg/about/the7categoriesofadditivemanufacturing/materialextrusion/>

/18/ Deep dive: Bound Metal Deposition. Desktop Metal Web Pages. Accessed 13.12.2019. <https://www.desktopmetal.com/article/deep-dive-bound-metal-deposition/>

/19/ Mark, G. 2017. A Revolutionary New Way to Manufacture Metal Parts. Markforged Web Pages. Accessed 13.12.2019. <https://markforged.com/blog/adam/>

/20/ AMpower. Additive Manufacturing webpage. Accessed 19.2.2020. <http://additivemanufacturing.com/2018/10/17/ampower-releases-new-study-examining-metal-additive-manufacturing/>

/21/ Metal Additive Manufacturing: An Introduction. Metal AM Web Pages. Accessed 13.12.2019 <https://www.metal-am.com/introduction-to-metal-additive-manufacturing-and-3d-printing/>

/22/ How Real Value of Metal Additive Manufacturing Can Be Leveraged for Automotive Production. 2018. Manufacturing Tomorrow Web Pages. Accessed 6.10.2019. <https://www.manufacturingtomorrow.com/article/2018/09/how-real-value-of-metal-additive-manufacturing-can-be-leveraged-for-automotive-production/12149>

/23/ The Business Value of Metal Additive Manufacturing. 2018. Digital Alloys Guide to Metal Additive Manufacturing – Part 1. Accessed 27.12.2019. <https://www.digitalalloys.com/blog/business-value-of-metal-additive-manufacturing/>

/24/ Magnien, S. Design for Additive Manufacturing. Sirris. 2015. Accessed 9.7.2019 <http://3ddeconference.com/wp-content/uploads/2015/05/Julien-Magnien-Sirris.pdf>

/25/ Khajavi, S., Holmström, J. & Partanen, J. 2018. Additive manufacturing in the spare parts supply chain: hub configuration and technology maturity. Rapid Prototyping Journal.

/26/ 3D Printing Media Network webpage. Accessed 19.2.2020. <https://www.3dprintingmedia.network/>

/27/ International Organization for Standardization Web Pages. Accessed 19.8.2019 <https://www.iso.org/home.html>

/28/ Schwenksystem mit Servoantrieb. Additive-Fertigung webpage. Accessed 19.2.2020 https://www.additive-fertigung.at/detail/schwenksystem-mit-servoantrieb_147328/

/29/ MarkForged Offers Mark One Composite Cloud-Based 3D Printer. TenLinks Web Pages. Accessed 12.10.2019 <http://www.tenlinks.com/news/markforged-offers-mark-one-composite-cloud-based-3d-printer/>

/30/ Markforged official Web Pages. Accessed 13.10.2019. <https://markforged.com/>

/31/ Boissonneault, T. 2018. Markforged announces shipment of 100th Metal X 3D printer. 3D Printing Media Network. Accessed 13.10.2019. <https://www.3dprintingmedia.network/markforged-100th-metal-x/>

/32/ Fisher-Wilson, G. 2019. 2019 Markforged Metal X: Review the Specs. All3DP Webpages. Accessed 29.10.2019 <https://all3dp.com/1/markforged-metal-x-review-3d-printer-specs/>

/33/ Brier, E. 2019. Next Billion – Dollar Startups News: 3-D Printing Startup Markforged Raises \$82 Million. Forbes Web Pages. Accessed 29.10.2019 <https://www.forbes.com/sites/elisabethbrier/2019/03/20/next-billion-dollar-startups-news-3-d-printing-startup-markforged-raises-82-million/>

/34/ Gonzales-Gutierrez, J., Cano, S., Schuschnigg, S., Kukla, C., Sapkota, J. & Holzer, C. 2018. Additive Manufacturing of Metallic and Ceramic Components by the Material Extrusion of Highly-Filled Polymers: A Review and Future Perspectives.

/35/ AKSteel Product Data Bulletin. 17-4 PH Stainless Steel.

/36/ Markforged Material Datasheet. 17-4 PH Stainless Steel.

/37/ Spencer O., Yusuf O. & Tofade T. 2018. American Journal of Mechanical and Industrial Engineering. Additive Manufacturing Technology Development: A Trajectory Towards Industrial Revolution. Metal AM Vol 3 No 2.

/38/ MarkForged Mark One – World’s First 3D Printer Designed to Print Continuous Carbon Fiber. AMazing Web Pages. Accessed 30.10.2019. <https://additivemanufacturing.com/2014/02/18/markforged-mark-one-worlds-first-3d-printer-designed-to-print-continuous-carbon-fiber/>

/39/ Miller-Stephenson Technical Data Sheet. 2016. Opteon Sion SF-79. Accessed 27.12.2019. <https://miller-stephenson.com/wp-content/uploads/2016/09/opteon-sion-specialty-cleaning-fluid-technical-information.pdf>

/40/ MicroCare Käyttöturvallisuustiedote. Tergo Metal Cleaning Fluid. Accessed 27.12.2019. <https://precisioncleaners.microcare.com/wp-content/uploads/2019/11/FI-BULK-TMCFEU-SDS20340.pdf>

/41/ Burd, T. 2019. Strategic Application Engineering Manager. Markforged. E-mail conversation.

/42/ / Wu, Y., German, R. M., Blaine, D., Marx, B. & Schlaefel, C. 2002. Effects of residual carbon content on sintering shrinkage, microstructure and mechanical properties of injection molded 17-4 PH stainless steel. *Journal of Material Science* 37, 3573-3583.

/43/ Spencer O., Yusuf O. & Tofade T. 2018. Additive Manufacturing Technology Development: A Trajectory Towards Industrial Revolution. *American Journal of Mechanical and Industrial Engineering* 3, 5, 80-90.

/44/ AMpower webpage. Accessed 19.2.2020. <https://am-power.de/>

/45/ Markforged Facilities Guide. 2019. Metal X System. Accessed 27.12.2019. https://s3.amazonaws.com/mf.product.doc.images/InternalKnowledge-Base/MetalX_Facilities_Guide.pdf

- /46/ Chemours Safety Data Sheet. 2019. Opteon SF79 Specialty Fluid. Accessed 27.12.2019. https://precision.w6wbbwn5-liquidwebsites.com/wp-content/themes/microcare_child/sds_sheets/United%20Kingdom/GB%20-%20BULK%20-%20SF79%20-%20SDS143913.pdf
- /47/ Ohjeita turvalliseen 3D-tulostukseen. Työterveyslaitos. Tietokortti 34. 2016. Accessed 27.12.2019. <https://www.ttl.fi/wp-content/uploads/2017/01/Ohjeita-turvalliseen-3D-tulostukseen.pdf>
- /48/ 3D-tulostuksen kemikaaliturvallisuus työpaikoilla. Työterveyslaitos. Malliratkaisu. 2016. Accessed 27.12.2019. <https://mb.cision.com/Public/5751/2134887/86ab1364ec6d8361.pdf>
- /49/ Nevalainen, H. 1979. Teräsopas. Helsinki. Teknillinen tarkastuskeskus.
- /50/ Salmi, T. 2010. Lujuusoppi. Tampere. Pressus Oy.
- /51/ Koivisto, K., Laitinen, E., Niinimäki, M., Tiainen, T., Tiilikka, P. & Tuomikoski, J. 2008. Konetekniikan materiaalioppi. Helsinki. Edita Prima Oy.
- /52/ Tensile test. Engineering Archives webpage. Accessed 19.2.2020. http://www.engineeringarchives.com/les_mom_tensiletest.html
- /53/ Azzam, A. & Li, W. 2014. An experimental investigation on the three-point bending behaviour of composite laminate. IOP Conference Series: Materials Science and Engineering.
- /54/ 3-point Flexura Test. Substances & Technologies webpage. Accessed 19.2.2020. http://www.substech.com/dokuwiki/doku.php?id=flexural_strength_tests_of_ceramics
- /55/ ISE316 Chapter 3 –Mechanics of materials. Accessed 19.2.2020. <https://slideplayer.com/slide/1596928/>

/56/ Metal X Design Reference Sheet. Markforged. 2018. Accessed 27.12.2019.
https://www.awp1.com/wp-content/uploads/2018/07/MetalXDesignGuide_V1-AWP.pdf

/57/ 2019 Markforged Metal X – Review the Specs. All3DP Webpages. Accessed 29.11.2019 <https://all3dp.com/1/markforged-metal-x-review-3d-printer-specs/>

/58/ Redwood, B., Schöffner F. & Garret, B. 2018. The 3D Printing Handbook.